EPR spectroscopic evidence of iron-catalysed free radical formation in chronic mountain sickness: Dietary causes and vascular consequences

Damian Bailey, Marcel Culcasi, Teresa Filipponi, Julien Brugniaux, Benjamin Stacey, Christopher Marley, Rodrigo Soria, Stefano Rimoldi, David Cerny, Emrush Rexhaj, et al.

EPR spectroscopic evidence of iron-catalysed free radical formation in chronic mountain sickness: dietary causes and vascular consequences

Damian M. Bailey[1], Marcel Culcasi[2], Teresa Filipponi[1], Julien V. Brugniaux[1,3], Benjamin Stacey[1], Christopher J. Marley[1], Rodrigo Soria[4], Stefano F. Rimoldi[4], David Cerny[4], Emrush Rexhaj[4], Lorenza Pratali[5], Carlos Salinas Salmòn[6], Carla Murillo Jáuregui[6], Mercedes Villena[6], Francisco Villafuerte[7], Antal Rockenbauer[8], Sylvia Pietri[2], Urs Scherrer[4,9] and Claudio Sartori[10]

[1]Neurovascular Research Laboratory, Faculty of Life Sciences and Education, University of South Wales, Wales, UK; [2]Aix Marseille Univ, CNRS, ICR, UMR 7273, Marseille, France; [3]HP2 Laboratory, INSERM U1300, Grenoble Alpes University, Grenoble, France; [4]Department of Cardiology and Biomedical Research, University Hospital, Bern, Switzerland; [5]Institute of Clinical Physiology, Pisa, Italy; [6]Instituto Bolivano de Biologia de Altura, La Paz, Bolivia; [7]Laboratorio de Fisiologı´a Comparada, Departamento de Ciencias Biolo´gicas y Fisiolo´gicas, Facultad de Ciencias y Filosofı´a, Universidad Peruana Cayetano Heredia. Lima, Péru; [8]Institute of Materials and Environmental Chemistry, Research Center for Natural Sciences, 1117 Budapest, Hungary; [9]Facultad de Ciencias, Departamento de Biología, Universidad de Tarapacá, Arica, Chile and [10]Department of Internal Medicine, University Hospital, UNIL-Lausanne, Switzerland

Keywords: chronic mountain sickness; free radicals; oxidative-nitrosative stress; systemic vascular function; oxidative catalysis

Running title: Redox-regulation of systemic vascular function in hypoxia

Trial registry: ClinicalTrials.gov; No: NCT01182792; URL: www.clinicaltrials.gov

Correspondence
Professor Damian Miles Bailey PhD FPVRI FRSC FACSM FTPS
Royal Society Wolfson Research Fellow
Director of the Neurovascular Research Laboratory
Alfred Russel Wallace Building
Faculty of Life Sciences and Education
University of South Wales
UK CF37 4AT

Telephone number: +44-1443-482296
Fax number: +44-1443-482285
*e*mail: damian.bailey@southwales.ac.uk
Webpage: http://staff.southwales.ac.uk/users/2240-dbailey1
Twitter: @USW_Oxygen
Orcid ID: 0000-0003-0498-7095

ABSTRACT

Chronic mountain sickness (CMS) is a high-altitude (HA) maladaptation syndrome characterised by elevated systemic oxidative-nitrosative stress (OXNOS) due to a free radical-mediated reduction in vascular nitric oxide (NO) bioavailability. To better define underlying mechanisms and vascular consequences, this study compared healthy male lowlanders (80 m, n = 10) against age/sex-matched highlanders born and bred in La Paz, Bolivia (3,600 m) with (CMS+, n = 10) and without (CMS-, n = 10) CMS. Cephalic venous blood was assayed using electron paramagnetic resonance spectroscopy and reductive ozone-based chemiluminescence. Nutritional intake was assessed via dietary recall. Systemic vascular function and structure were assessed via flow-mediated dilatation, aortic pulse wave velocity and carotid intima-media thickness using duplex ultrasound and applanation tonometry. Basal systemic OXNOS was permanently elevated in highlanders (P = <0.001 vs. lowlanders) and further exaggerated in CMS+, reflected by increased hydroxyl radical spin adduct formation (P = <0.001 vs. CMS-) subsequent to liberation of free ‘catalytic’ iron consistent with a Fenton and/or nucleophilic addition mechanism(s). This was accompanied by elevated global protein carbonylation (P = 0.046 vs. CMS-) and corresponding reduction in plasma nitrite (P = <0.001 vs. lowlanders). Dietary intake of vitamins C and E, carotene, magnesium and retinol were lower in highlanders and especially deficient in CMS+ due to reduced consumption of fruit and vegetables (P = <0.001 to 0.028 vs. lowlanders/CMS-). Systemic vascular function and structure were also impaired in highlanders (P = <0.001 to 0.040 vs. lowlanders) with more marked dysfunction observed in CMS+ (P = 0.035 to 0.043 vs. CMS-) in direct proportion to systemic OXNOS (r = -0.692 to 0.595, P =

<0.001 to 0.045). Collectively, these findings suggest that lifelong exposure to iron-catalysed systemic OXNOS, compounded by a dietary deficiency of antioxidant micronutrients, likely contributes to the systemic vascular complications and increased morbidity/mortality in CMS+.

1. INTRODUCTION

Chronic mountain sickness (CMS) is a high-altitude (HA) maladaptive syndrome that affects between 5-10% of the world's estimated 140 million highlanders who permanently reside >2,500 meters above sea-level [1]. It is characterised by excessive erythrocytosis (EE) and severe hypoxemia, frequently associated with moderate to severe pulmonary hypertension, that in advanced cases may evolve to cor pulmonale, congestive heart failure and stroke [2]. Currently, there are no effective long-term treatments given its complex pathogenesis.

It is well recognized that CMS associates with pulmonary vascular dysfunction [2], with emerging evidence indicating that the systemic circulation may be equally compromised, further compounding disease risk and premature mortality. In support, more marked impairments in flow-mediated dilation (FMD) and elevations in vascular stiffness and carotid intima-media thickness (cIMT) have been observed in comparatively more hypoxemic CMS patients (CMS+) compared to healthy well-adapted highlander (CMS-) and lowlander (sea-level) controls [3-6].

While preliminary evidence supports a contributory role for an exaggerated and sustained elevation in basal systemic oxidative-nitrosative stress (OXNOS) subsequent to enhanced free radical-mediated scavenging of vascular nitric oxide (NO) bioavailability [3, 7], the contributing species, underlying mechanisms and functional significance remain obscure. Cellular hypoxia has consistently been shown to promote mitochondrial superoxide ($O_2^{\cdot-}$) formation primarily from complex III in vitro [8], due to a Na^+-mediated reduction in mitochondrial inner membrane fluidity resulting in the entrapment and accumulation of ubisemiquinone at the Qo site [9]. Subsequent

formation of hydrogen peroxide (H_2O_2) can diffuse rapidly into the cytoplasm, facilitated by a reduction in mitochondrial matrix and intermembrane space peroxidase activities [10] to initiate extracellular 'blood-borne' lipid peroxidation, that in the presence of 'free' ferrous (Fe^{2+}) iron (see below) can give rise to secondary lipid-derived alkoxyl ($LO^{\bullet}$) and alkyl ($LC^{\bullet}$) radicals [11]. Intravascular $O_2^{\cdot-}$ can also be generated from extra-mitochondrial sources including nicotinamide adenine dinucleotide phosphate- and xanthine oxidases, cytochrome *P*-450 enzymes, lipoxygenases, phagocytes and hydrogen ion formation subsequent to hypoxia-induced metabolic acidosis [12-14]. These radical species are all thermodynamically capable of initiating additional chain reactions ($LO^{\bullet}/LC^{\bullet}$ + L-H → $L^{\bullet}$) [15] and reacting directly with intravascular NO at diffusion-controlled rates (k = ~10^9 M/s) to yield peroxynitrite ($O_2^{\cdot-}/LO^{\bullet}/LC^{\bullet}$+ NO → $ONOO^-$) [16] that in turn can mediate lipid peroxidation/protein tyrosine nitrosylation and uncouple endothelial NO synthase [13].

However, to what extent $O_2^{\cdot-}$ formation proceeds directly in vivo including the potential for reductive formation of Fe^{2+} (Eq. 1) capable of catalysing Fenton (Eq. 2) and Haber-Weiss (Eq. 3)-induced generation of hydroxyl radicals (HO•) has not previously been investigated. Overall, these biological pathways predominantly reflect a transition metal catalysed reaction stemming from Fridovich's original $O_2^{\cdot-}$ theory of O_2 toxicity, given that the Haber-Weiss reaction (Eq. 3) has a negligible rate constant [17].

$$Fe^{3+} + O_2^{\cdot-} \rightarrow Fe^{2+} \qquad (1)$$

$$Fe^{2+} + H_2O_2 \rightarrow HO\bullet + OH^- + Fe^{3+} \qquad (2)$$

$O_2^{\cdot-} + H_2O_2 \rightarrow O_2 + HO\bullet + OH^-$ (3)

Furthermore, to what extent dietary deficiency of antioxidant micronutrients due to inadequate consumption of fruit and vegetables (F+V) further compounds systemic OXNOS is equally unknown, despite preliminary evidence for lower circulating concentrations of ascorbate and α/ß-carotene in CMS+ [3].

To address these limitations, the present study combined electron paramagnetic resonance (EPR) spectroscopy with ozone-based chemiluminescence (OBC) for the direct detection and molecular characterisation of OXNOS biomarkers, to test the following hypotheses. First, Me-β-cyclodextrin (MeβCD)-assisted spin trapping with the novel stereoselective phosphorylated nitrone, 2-methyl-2-(5,5-dimethyl-2-oxo-1,3,2-dioxaphosphinan-2-yl)-3,4-dihydro-2H-pyrrole 1-oxide (Me_2CyDEPMPO), would demonstrate more marked elevations in systemic $O_2^{\cdot-}$ and HO• formation in CMS+ relative to healthy lowlander and CMS- controls specifically related to increased catalytic (‘free’) iron bioavailabilty. Second, this would be related to inadequate intake of antioxidant micronutrients as a consequence of lower F+V consumption. Third, exaggerated OXNOS would be associated with more marked impairments in systemic vascular function and structure extending prior observations [3, 7] given its more informed mechanistic basis.

2. METHODS

2.1. Ethics

The experimental protocol was approved by the Institutional Review Boards for Human Investigation at the University of San Andres, La Paz, Bolivia (CNB #52/04), Universidad Peruana Cayetano Heredia, Lima, Péru (#101686), University of Lausanne, Lausanne, Switzerland (#89/06, #94/10), and University of South Wales, Pontypridd, UK (#4/07), prior to registration in a clinical trials database (clinicaltrials.gov; Identifier: NCT01182792). All procedures adhered to the guidelines set forth in the Declaration of Helsinki and participants provided written informed consent following explanation of the purposes of clinical experimentation and risks involved.

2.2. Design

We conducted a cross-sectional, population-based, observational study in accordance with the STROBE statement [18]. The Neurovascular Research Laboratory in the UK (~80 m) and Instituto Boliviano de Biologia de Altura in La Paz, Bolivia (~3,600 m) were the primary sites of investigation. Select aspects of the cardiopulmonary data have previously been published as part of a wider investigation focused exclusively on the mechanisms underlying cerebrovascular dysfunction in CMS+ [7]. Thus, although the present study adopted an identical experimental design, it constitutes an entirely separate question with additional experimental measures of free radicals, catalytic iron, dietary intake and systemic vascular function and structure. Fig. 1 provides a schematic summary of the experimental design.

2.3. Participants

For all participants, inclusion criteria specified that they were born and had lived permanently at their resident altitude and were sedentary, defined as no formal recreational activity outside of everyday living [19]. Exclusion criteria included those with significant developmental delay or learning difficulties, diagnosis of any central neurological disease such as aneurysm, stroke, transient ischemic attack, epilepsy, multiple sclerosis and psychiatric disorders including any history of traumatic brain injury and hypertension. None of the participants were taking nutritional supplements including over-the-counter antioxidant or anti-inflammatory medications. We specifically chose to focus on males given their higher prevalence of CMS notwithstanding our inability to control for differences in circulating estrogen known to impact redox-regulation of systemic vascular function in females. Prior to inclusion, all participants were subject to an extensive clinical examination that consisted of a thorough medical history, chest auscultation and 12-lead ECG. Participants were subsequently familiarised with the equipment and all experimental procedures.

2.3.1. Highlanders

We recruited 10 male patients with primary CMS (CMS+) and 10 healthy age- and education-matched controls without CMS (CMS-) native to La Paz, Bolivia (Table 1). Symptoms of CMS were scored and clinical diagnosis confirmed by an excessive erythrocytosis including hemoglobin (Hb) > 20 g/dL in the presence of normal pulmonary function and no history of working in the mining industry [1]. All participants identified themselves as Aymaras and were from similar socio-economic backgrounds

having been born and bred in La Paz (Cerro de Pasco for secondary study) with Spanish spoken as their first language.

2.3.2. Lowlanders

We recruited 10 age and education matched healthy Caucasian males in the UK (Table 1) who were all born and bred close to sea-level with no prior history of ascending above 1,500 m.

2.4. Socioeconomic status (SES)

In addition to educational attainment (completed Secondary School/University) for the purposes of group matching, we also assessed occupational prestige using established methods that employed the 1989 modification of scores taken from the original 1980 US Census Occupational Category [20]. In brief, published scores (highest reflecting most prestigious occupation) were assigned to individual occupational titles classified under the following (nine) general categories: managerial and administrative, professional specialty, technical, sales, administrative support, service, farming/ forestry/fishing, precision production/craft/repair, and laborer.

2.5. Cardiopulmonary assessments

A lead II electrocardiogram (Dual BioAmp; ADInstruments Ltd, Oxford, UK) was used to measure heart rate (HR). Finger photoplethysmography (Finometer PRO, Finapres Medical Systems, Amsterdam, The Netherlands) was used to measure beat-by-beat arterial blood pressure for calculation of mean arterial pressure (MAP), stroke volume

(SV) and cardiac output (Q̇) using the Modelflow algorithm [21] that incorporates participant sex, age, stature and mass (BeatScope 1.0 software; TNO; TPD Biomedical Instrumentation, Amsterdam). End-tidal partial pressures of oxygen and carbon dioxide ($PET_{O2/CO2}$) were determined from a leak-free mask and analysed via capnography (ML 206, ADInstruments). Pulse oximetry (Nonin 9550 Onyx II, Nonin Medical, Inc., Plymouth, MI, USA) was employed to determine arterial oxyhemoglobin saturation (SaO_2) on the third digit of the right hand. Beat-by-beat data were continuously recorded at 1 kHz using an analog-to-digital converter (Powerlab/16SP ML795; ADInstruments, Colorado Springs, CO, USA) stored on a personal computer for off-line analysis (LabChart version 7.2.2, ADInstruments).

2.6. Metabolic assessments

Participants were asked to refrain from physical activity, caffeine and alcohol and maintain their normal dietary behaviors before and during formal experimentation. They were 12 h overnight fasted when they attended the laboratory at 8 am. We obtained blood samples without stasis following 20 min of seated rest to control for the confounds associated with plasma volume shifts.

2.6.1. Chemicals

All chemicals including dimethylsulfoxide (DMSO), MeβCD (CAS 128446-36-6), diethylenetriaminepentaacetic acid (DTPA), desferrioxamine mesylate (DFX), ferric chloride ($FeCl_3$), ferrous sulfate ($FeSO_4$), H_2O_2 and the spin trap *N-tert*-butyl-α-phenylnitrone (PBN) were of the highest available purity from Sigma-Aldrich. The spin

trap Me_2CyDEPMPO, a cyclic analogue of 5-diethoxyphosphoryl-5-methyl-1-pyrroline 1-oxide (DEPMPO; see Fig. 1 inset), was synthesised according to [22].

2.6.2. Blood sampling

Blood was obtained from an indwelling cannula located in a cephalic vein into Vacutainers® (Becton, Dickinson and Company, Oxford, UK). Centrifugation was performed at 600g (4° C) for 10 min to yield hemolysis-free supernatant [11]. Plasma samples were decanted directly into cryogenic vials (Nalgene® Labware, Thermo Fisher Scientific Inc, Waltham, MA, USA) and immediately snap-frozen in liquid nitrogen (N_2) and shipped/stored under N_2 gas (Cryopak, Taylor-Wharton, Theodore, AL, USA) prior to analysis in the UK. Samples were left to defrost at 37 °C in the dark for 5 min prior to batch analysis.

2.6.3. Free radicals

X-band EPR spectra were recorded at room temperature using a Bruker (Karlsruhe, Germany) EMX spectrometer, except for studies with Me_2CyDEPMPO where a Bruker ESP 300 spectrometer was used. Throughout, 100 kHz modulation frequency, 10 or 20 mW microwave power (MP) and a standard TM_{110} cavity were used.

2.6.3.1. **Preliminary in vitro EPR controls**

In order to assist the assignments of Me_2CyDEPMPO adducts detected ex vivo in the blood of participants (see Results section), in vitro tests were performed in the presence of an excess of MeβCD. This cyclodextrin (Fig. S1, inset; Supplementary data) was

included in the spin-trapping milieu on the basis of the reported formation of cyclodextrin-guest inclusion complexes with DEPMPO spin adducts that yield increased stability toward bioreductive EPR silencing mechanisms in buffers [23] and cells [24]. In addition, these preliminary experiments, using a Fenton driven HO• generator, determined to what extent MeβCD interferes quantitatively with (i) formation of the Me_2CyDEPMPO/HO• spin adduct (Me_2CyDEPMPO-OH) in phosphate buffer solution (PBS, pH 7.4) and (ii) formation of Me_2CyDEPMPO/methyl radical spin adduct (Me_2CyDEPMPO-Me) when the generator used in (i) was run in the presence of the competitive inhibitor DMSO, supplemented in the buffer. A typical Me_2CyDEPMPO-OH control generating system in PBS (20 mM) for experiments (i) contained Me_2CyDEPMPO (30 mM), H_2O_2 (1 mM), with final addition of $FeSO_4$ (1 mM) to catalyse HO• formation. In these systems MeβCD (50 mM) was added to (i) 30 s before or after addition of iron salt. In Me_2CyDEPMPO-Me generating experiments, MeβCD (50 mM) was added before iron to the milieu described in (i), that also contained DMSO (10% v/v). Samples were placed in 50 µL glass capillary tubes (Hirschmann Laborgeräte, Germany) and sealed with Critoseal®. Single-scan EPR spectra were sequentially recorded 1–18 min following addition of iron salt with the following parameters: MP, 10 mW; magnetic field resolution (R), 2048 points; modulation amplitude (MA), 0.521 G; receiver gain (RG), 2×10^5; time constant (TC), 81.92 ms; sweep rate (SR), 1.55 G/s for a sweep width (SW) of 130 G.

2.6.3.2. Ex-vivo EPR studies in blood

Three experiments were performed for the molecular detection and characterisation of free radicals in blood.

[i] ***MeβCD-assisted spin-trapping on Me$_2$CyDEPMPO:*** Heparinised whole blood samples (1 mL) were obtained from all participants and placed into 2 mL cryovial tubes pre-filled with a mixture of (final concentration) 0.2 mM DTPA, 80 mM MeβCD, 40 mM PBS and 0.5 mL of aqueous Me$_2$CyDEPMPO (0.1 M), and immediately frozen in liquid N_2. EPR acquisition in glass capillaries was initiated 1 min after complete thawing with the same parameters as for preliminary tests above, except that 2 cumulative scans were averaged due to low signal-to-noise ratio. In both in vitro and ex vivo experiments using Me$_2$CyDEPMPO, relative spin adduct concentrations were derived from the simulated spectra [25] and the unequivocal assignment of *trans/cis*-Me$_2$CyDEPMPO-OH and *trans*-Me$_2$CyDEPMPO-Me adducts (see Fig. 2A, with R = Me) was based on the close similarity (< 5%) of their calculated EPR hyperfine couplings (hfcs) with those reported earlier using the same free radical generators in buffer [22].

PBN spin trapping and catalytic iron experiments were conducted in a random subsample of 5 CMS+ patients to provide additional 'proof-of-concept' insight into the mechanisms underlying Me$_2$CyDEPMPO-OH adduct(s) formation (see Limitations).

[ii] ***Spin-trapping*** **using** ***PBN:*** Whole blood (4.5 mL) was added to a 6 mL glass vacutainer (SST) primed with 1.5 mL of cold freshly prepared PBN dissolved in physiological saline (50 mM final concentration). The vacutainer was gently mixed then placed in the dark to clot for 10 min. Following centrifugation, 1.5 mL of the serum-adduct was removed, flash-frozen and stored in liquid N_2 prior to batch analysis. During

the analysis, samples were thawed on ice and 1 mL of the serum-adduct was added to a boro-silicate glass tube containing 1 mL of spectroscopic grade toluene and vortex-mixed for 10 s. The sample was centrifuged for a further 10 min and 200 µL of the organic supernatant added to a (N_2-flushed) precision-bore quartz EPR tube and vacuum-degassed to remove O_2 prior to EPR spectroscopy. All sample handling was performed in a darkened room to minimise photolytic degradation. Instrument settings were: MP, 20 mW; R, 4096 points; MA, 0.5 G; RG, 1.0×10^5; TC, 82 ms; SW, 50 G, for 10 cumulative scans.

[iii] ***Catalytic iron:*** Additional EPR measurements were performed on the same blood samples as in (ii). The basic principle of the assay, which relies on relative changes in the EPR signal intensity of the persistent ascorbate radical $A^{\cdot-}$ (yielding an EPR doublet with a_H ~1.76 G; Fig. 3) during air auto-oxidation of ascorbate, has been used for probing catalytic iron ex vivo [26]. Briefly, separate vials of serum (200 µL) were treated with 500 µM (final concentration) of DFX (reduces iron-catalysed oxidation) and 10 µM of $FeCl_3$-EDTA (stimulates iron catalysed oxidation). Instrument settings were: MP, 20 mW; R, 4096 points; MA, 2.0 G; RG, 1.0×10^5; TC, 41 ms; SW, 10 G, for 15 cumulative scans. Spectra were filtered identically using Bruker WinEPR version 2.11 software and simulated using Bruker SimFonia or SimEPR32 (Bruker Biospin) [27]. Relative free radical concentrations were calculated by double integration of simulations using Origin 8 software (OriginLab Corp., Northampton, MA, USA). We also chose to 'normalise' $A^{\cdot-}$ formation for differences in ambient ascorbate concentrations. Following deproteination

with 10% metaphosphoric acid, ascorbate was assayed via fluorimetry based on the condensation of dehydroascorbic acid with 1,2-phenylenediamine [28].

2.6.4. Protein carbonyls (PC)

Plasma was diluted with 4 vol of PBS 0.1X prior to analysis and 100 µL placed in 96-well microplates and left to react for 15 min at 21ºC with an aliquot (100 µL) of the NBDH assay solution (Carbofax®, Yelen Analytics, Marseille, France) [29]. Concentration of NBDH-reacted PC was determined by fluorescence (emission determined at 560 nm using an excitation wavelength at 480 nm) with reduced/oxidized bovine serum albumin employed as calibrants. The concentration of PC was calculated relative to total protein content, the latter determined using the Pierce BCA protein assay kit (Fisher Scientific, France). Intra- and inter-assay CVs were <10%.

2.6.5. NO metabolites

Plasma NO metabolites were measured via reductive ozone-based chemiluminescence (Sievers NOA 280i, Analytix Ltd, Durham, UK) [30]. Plasma (200 µL) was injected into tri-iodide reagent for the combined measurement of nitrite and *S*-Nitrosothiols (NO_2^- + RSNO). A separate sample (400 µL) was mixed with 5% acidified sulphanilamide (9:1) and left to incubate in the dark at 21 ºC for 15 min to remove NO_2^- prior to injection into tri-iodide reagent for the direct measurement of RSNO. Plasma NO_2^- was subsequently calculated as (NO_2^- + RSNO) - RSNO. Total NO bioactivity was calculated as the cumulative concentration of all metabolites. Signal output was plotted against time using Origin 8 software and smoothed using a 150-point averaging algorithm. The Peak

Analysis package was used to calculate the area under the curve and subsequently converted to a concentration using standard curves of sodium NO_2^-. Intra- and inter-assay CVs for all metabolites were <10%.

2.6.6. Iron metabolites

Iron metabolism was assessed in a separate group of age-matched lowlanders/highlanders given ethical constraints imposed during blood volume sampling in the primary study. Serum iron and transferrin were measured using a colorimetric and immunoturbidimetric assay respectively via the C501 module on a Cobas 6000 analyzer (Roche) (32). Serum ferritin was determined using an electrochemiluminescence immunoassay using a Cobas e601 module (Roche). Assuming that 1 mol of transferrin (molecular mass 79,570 Da) has the capacity to bind two atoms of iron (atomic mass 56), transferrin saturation (TSAT) was calculated as:

$$\text{TSAT (\%)} = \frac{\text{Serum iron (µg/dL)}}{\text{Transferrin (mg/dL)}} \times 70.9 \text{ [31]}$$

Total iron binding capacity (TIBC) was calculated as:

TIBC = (µg/dL) = Transferrin (mg/dL) × 1.41 [31]

2.8. Dietary analysis

Nutritional intake was assessed using the 24 h dietary recall (24-HDR) method conducted on two separate days [32]. The 24-HDR is considered the least biased structured self-report instrument that is the most accurate for low income populations [33, 34]. Participants were asked to provide detailed information about the food and beverages consumed including preparation methods, ingredients used, amount consumed, leftover, brand name of commercial products, time of the day and type of

meal. Standard household measuring tools, food models, photos and other visual aids were also employed to help judge and estimate portion size in order to improve accuracy. Dietary data were analyzed using NetWISP dietary analysis software (Version 4.0, Tinuviel Software; Anglesey, UK).

2.8. Vascular assessments

All resting measurements were performed following 10 min of supine rest, breathing room air at each respective location at the prevailing barometric pressures (normoxic normocapnia for lowlanders, hypoxic hypocapnia for highlanders).

2.8.1. Systemic arterial function

Systemic conduit artery endothelial function was assessed by determining the increase of the brachial artery (BA) diameter evoked during reactive hyperemia using high-resolution ultrasound and automatic wall tracking software [35] according to International Guidelines [36]. Briefly, the BA was identified approximately 5 cm above the antecubital fossa with high-resolution duplex ultrasound (Acuson Sequoia C512, Acuson Siemens, Mountain View, CA, USA or Esaote MyLab30 Gold, Genova, Italy) and a high frequency (7-10 MHz) linear array probe. The ultrasound probe was fixed in a stereotactic clamp (AMC Vascular Imaging, Amsterdam) and flow recorded continuously throughout. After 1 min of baseline measurements, a pressure cuff placed around the forearm was inflated to 250 mmHg for 5 min. Following cuff-deflation, the hyperemia-induced changes in BA diameter and flow were continuously monitored for 3 min. B-mode ultrasound images were analysed with a validated system for automatic

real-time measurement of BA diameter (FMD Studio, Computer Vision Group, Pisa, Italy) [37]. Flow-mediated dilation (FMD) was expressed as the maximal percentage change in BA diameter from baseline and allometrically scaled (adjusted FMD) to account for differences in baseline BA diameter [38]. Endothelium-independent dilation was assessed by measuring the percentage increase in BA diameter to an acute oral dose (250 µg) of glyceryl trinitrate (GTN; UCB-Pharma SA). The intra-observer CV was <5%.

2.8.2. Systemic arterial stiffness

In accordance with International Guidelines [39], large artery stiffness was assessed non-invasively via the carotid-femoral pulse wave velocity (PWV) using the Complior® device (Artech Medical, Pantin, France) [39, 40]. Briefly, common carotid and femoral arterial pressure waveforms were recorded simultaneously with mechano-transducers. The mean wave transit time for 10 heart beats was calculated by the system software using the foot-to-foot method. To determine aortic PWV (aPWV), the surface distance between the recording sites was determined with a flexible tape measure. Central pulse wave analysis was performed non-invasively using the SphygmoCor® system (AtCor Medical Pty Ltd, Sydney, Australia). The radial artery pressure waveform was recorded at the wrist using applanation tonometry with a high-fidelity micromanometer (SPT-301, Millar Instruments, Houston, TX, USA) and the central (ascending aortic) pressure waveform derived using a validated transfer function [41]. AIx was calculated as the difference between the 1st and 2nd peaks of the central arterial waveform, expressed as

a percentage of the pulse pressure (PP) and normalised to 75 b/min heart rate (AIx-75) [42]. The intra-observer CV for all metrics was <5%.

2.8.3. Systemic arterial structure

Duplex ultrasound scanning of the right and left common carotid arteries (CCA), carotid bifurcations and the origin of the internal carotid arteries was performed in conjunction with simultaneous ECG acquisition in participants placed supine with slight hyperextension of the neck at 45º. The right and left carotid arteries were imaged in the anterolateral, posterolateral and mediolateral planes, 1–2 cm proximal to the carotid bulb to identify the optimal angle of incidence [43, 44]. Radiofrequency signals with a 21 μm resolution (RF QIMT, Esaote, Genova, Italy) were employed to measure cIMT. After scanning the vessel, each radiofrequency line was automatically analysed forward and backward in real time by the echo-device at a site free of any discrete plaque. The mean of 3 measures from the right and 3 from the left carotid artery was documented. The intra-observer CV was <5%.

2.9. Statistical analysis

2.9.1. Power calculation

Prospective power calculations were performed using G* Power 3.1 software. Given the lack of pilot data in Me_2CyDEPMPO-adducts in CMS+/CMS-, we focused on baseline differences in (absolute) FMD and aPWV based on our prior research. Assuming comparable differences and corresponding effect sizes (η = 0.51 for FMD and 0.55 for

aPWV), we required a total sample size ranging from 12−15 participants (4−5 per group) to achieve a power of 0.80 at $P < 0.05$. We chose to further inflate to a total sample size of 30 (10 per group) to accommodate potential data loss (prospective power of >0.95).

2.9.2. Inferential statistics

Data were analysed using using the Statistics Package for Social Scientists (IBM SPSS Statistics V 28.0). Shapiro-Wilk *W* tests ($P > 0.05$) confirmed that all data sets were normally distributed. Demographic (Table 1), dietary (Table 2), and metabolic (Table 3) data were analysed using one-way analyses of variance (ANOVA) and *post-hoc* Bonferonni-adjusted independent samples *t*-tests assuming a main effect was observed. Relationships between variables were assessed using Pearson Product Moment Correlations. Significance was established at $P < 0.05$ for all two-tailed tests (with individual P values for all comparisons shown) and data expressed as mean ± standard deviation (SD).

3. RESULTS

3.1. Demographics

By design, groups were of a similar age and educational attainment, whereas highlanders, in particular CMS+, were more hypoxemic, hypocapnic and erythrocytotic (Table 1). Despite comparable body mass, CMS+ were generally shorter with a corresponding higher BMI and waist-to-hip ratio (Table 1). Resting HR, SV and $\dot{Q}$ were generally elevated and PET_{O2}, PET_{CO2}, DBP and TPR were lower in the highlanders (Table 1). No between differences were observed in any of the SES metrics including occupational prestige scores (Table 1).

3.2. Metabolic assessments

3.2.1. In vitro studies (quality control)

3.2.1.1. MeβCD does not affect Me_2CyDEPMPO spin adduct formation in vitro

Trapping of Fenton-derived HO• on Me_2CyDEPMPO (30 mM) in plain PBS yielded a primary symmetrical 14-lined EPR spectrum with calculated hfcs consistent with a mixture of *trans*-Me_2CyDEPMPO-OH (*trans*-OH; a_N = 13.94 G, a_P = 48.89 G, a_H^{β} = 12.40 G) and *cis*-Me_2CyDEPMPO-OH (*cis*-OH; a_N = 13.93 G, a_P = 50.59 G, a_H^{β} = 14.08 G) diastereoisomers (Fig. 1B) [17]. A small contaminant Me_2CyDEPMPO/alkyl radical adduct (Fig. 1B; a_N = 14.46 G, a_P = 50.79 G, a_H^{β} = 20.86 G; ~10% of the total signal), likely a decomposition nitroxide, was also detected. A typical signal recorded 2 min after HO• formation was triggered is illustrated in Fig. S1A (Supplementary data). Strikingly, inclusion of excess MeβCD (50 mM) in the above [Fenton + nitrone] system yielded mixtures of *trans*-OH, *cis*-OH and alkyl spin adducts with EPR spectra retaining similar

shapes and hfcs within experimental accuracy (Fig. S1B, C and Table S1; Supplementary data). This implies a general lack of coordination between MeβCD and these spin adducts that would typically yield distorted EPR signals characteristic of the superimposition of free and complexed radicals, as reported for the DEPMPO/superoxide (-OOH) adduct [19]. However, a near two-fold decrease in the total EPR signal was observed when MeβCD was present before vs. after Fenton-induced Me_2CyDEPMPO-OH formation, reflecting competitive 'side attack' of HO• on the MeβCD backbone forming non-spin-trapped radicals (Fig. S1; Supplementary data). Accordingly, pre-inclusion of MeβCD in a [Fenton + DMSO] system also resulted in a loss of intensity for the expected *trans*-Me_2CyDEPMPO-Me signal [17], with formation of a strong unassigned alkyl adduct that may have originated from the MeβCD structure (Fig. S1D; Supplementary data).

3.2.1.2. Stability of Me_2CyDEPMPO adducts and trans-OH/cis-OH ratios

All spin adduct concentrations decreased progressively with time (up to 15 min after iron added), with no clear influence of MeβCD (Fig. 2SA, B; Supplementary data). Signal acquisitions started 1 min after thawing of the sample given that we anticipated weak EPR signals in blood [Me_2CyDEPMPO+MeβCD]. Here, *trans*/*cis* ratios recorded after 2 min of continuous Fenton-mediated HO• formation were in general agreement with the published value of 1.4 (AU) observed in the same conditions for a stopped Fenton reagent [22], except when CD was added before the Fenton reaction, where the ratios were considerably higher (Fig. S2C; Supplementary data).

3.2.2. Ex vivo studies (clinical experimentation)

3.2.2.1. Me_2CyDEPMPO spin-trapping in the presence of MeβCD

Unlike lowlanders (no adducts detected), highlander blood was paramagnetic and consistently exhibited either a single component consistent with a Me_2CyDEPMPO-alkyl adduct (i.e., having a_H ~20 G; all CMS-, all CMS+) or combination of *cis/trans*-Me_2CyDEPMPO-OH and -alkyl adducts (one CMS-, all CMS+). In combination with the in vitro controls (above), all EPR spectra in blood were satisfactorily simulated assuming that no penetration of spin adducts in the inner cavity of CD occurred. Representative EPR spectra obtained from a (single) lowlander, CMS- participant and CMS+ patient with simulated composite adducts and relative intensities are illustrated in Fig. 2B. The group signal intensities of total and composite Me_2CyDEPMPO-OH adducts (no difference in -alkyl adducts) were consistently higher in CMS+ (Fig. 2C) representing 8 ± 25% (CMS-) vs. 45 ± 18% (CMS+, P = 0.001) for Me_2CyDEPMPO-OH and 92 ± 25% (CMS-) vs. 55 ± 18% (CMS+, P = 0.001) Me_2CyDEPMPO-alkyl adducts respectively, of the total signal intensities recorded. The *trans:cis* ratios for CMS- was 1.427 AU (n = 1) and 1.741 ± 0.266 (1.151-2.125) AU for CMS+.

3.2.2.2. PC

Baseline PC were higher in CMS+ compared to CMS- (Fig. 2D).

3.2.2.3. Catalytic iron

Compared to control (untreated) samples, DFX decreased $A^{\cdot-}$ by 30 ± 12% (P = 0.029) whereas Fe(III)-EDTA increased $A^{\cdot-}$ by 125 ± 17% (P = 0.002). Differences persisted following correction for ambient ascorbate (Fig. 3 A, B).

3.2.2.4. PBN spin-trapping

We observed EPR sextets from toluene-extracted blood samples with a primary signal that was consistent with an alkoxyl adduct (PBN-OR: a_N = 13.59 G; a_H^{β} = 1.85 G, Fig. 3 C, D).

3.2.2.5. NO metabolites

Total bioactive NO was consistently suppressed in highlanders due to lower NO_2^- whereas no differences were observed in RSNO (Fig. 4A). Both NO_2^- and RSNO were comparable between CMS+ and CMS- (Fig. 4A).

3.2.2.6. Iron metabolism (sub-study)

No between group differences were observed in total iron, ferritin, transferrin, TSAT or TIBC (Table S2; Supplementary data).

3.3. Dietary intake

Caloric and macronutrient (protein, carbohydrate, fat and fiber) intake were comparable across groups and generally consistent with current recommendations (Table 2). In

contrast, F+V consumption was markedly lower in highlanders resulting in a reduced intake of vitamins C and E, carotene, magnesium and retinol compared to lowlanders (Table 2). The lower vegetable and vitamin C intake was more pronounced in CMS+ compared to CMS- (Table 2).

3.4. Vascular assessments

3.4.1. Function

Baseline BA diameters were similar across groups (Table 3). Absolute and adjusted FMD were consistently lower in highlanders, although no differences were observed between CMS+ and CMS- (Table 3). In contrast, GTN-induced dilation was lower in CMS+ compared to CMS- (Table 3), although there was a tendency for baseline BA diameter to be higher (4.69 ± 0.55 mm vs. 4.27 ± 0.32 mm, P = 0.086).

3.4.2. Stiffness

Central SBP was consistenly higher and central DBP lower in highlanders, whereas no differences were observed between CMS+ and CMS- (Table 3). In contrast, aPWV was elevated in highlanders and greater in CMS+ compared to CMS- (Table 3). No between group differences were observed in AIx-75 (Table 3).

3.4.3. Structure

Elevated cIMT was observed in CMS+ compared to CMS- (Table 3).

3.5. Correlational analyses

3.5.1. Me_2CyDEPMPO adducts, NO_2^- and CMS

Inverse relationships were observed between Me_2CyDEPMPO-alkyl and NO_2^- (Fig. 5 A) and FMD (Fig. 5 B) in CMS+. A positive relationship was observed between (total) Me_2CyDEPMPO-OH/alkyl adducts and CMS scores (Fig. 5 C) in the highlanders (pooled CMS- and CMS+).

3.5.2. NO_2^- and vascular function

In all participants (pooled Lowlanders, CMS- and CMS+), a positive relationship was observed between NO_2^- and absolute FMD (Fig. 5 D) with inverse relationships between NO_2^- and aPWV (Fig. 5 E) and AIx-75 (Fig. 5 F).

4. DISCUSSION

The present study has identified three important findings that extend our understanding of redox-regulated mechanisms underlying lifelong mal/adaptation to HA. First, basal systemic OXNOS was permanently elevated in highlanders and further exaggerated in CMS+. This was reflected by elevated global protein carbonylation implying increased oxidation and HO• formation subsequent to liberation of 'free' catalytic iron consistent with a Fenton and/or NA mechanism(s), coupled with lower NO_2^-. Second, this was accompanied by inadequate intake of select antioxidant micronutrients due to lower F+V consumption. Third, we confirm that systemic vascular function and structure were collectively more impaired in CMS+ in direct proportion to the systemic OXNOS response. Collectively, these findings are the first to suggest that lifelong exposure to iron-catalysed systemic OXNOS, compounded by a dietary deficiency of antioxidant micronutrients, likely contributes to the systemic vascular complications and increased morbidity/mortality in CMS+.

4.1 Systemic OXNOS and iron catalysis

We specifically employed EPR spin-trapping with Me_2CyDEPMPO to optimise detection of blood-borne $O_2^{\cdot-}$ and HO• given short half-lives and established roles in regulating vascular endothelial function either directly or through secondary formation of reactive oxygen/nitrogen species [45]. We also chose to include an excess of MeβCD in the trapping milieu to further improve adduct stability by forming inclusion complexes that protect against ascorbate, α-tocopherol and glutathione-induced bioreduction to EPR 'silent' hydroxylamines [23, 24]. Importantly, control experiments confirmed that MeβCD

did not affect Me_2CyDEPMPO spin adduct formation in vitro, yet despite our best efforts, we consistently failed to detect Me_2CyDEPMPO-OOH adducts in participants' blood.

In contrast, highlander blood exhibited paramagnetic spectra consistent with *cis/trans*-Me_2CyDEPMPO-OH and/or -alkyl adducts with the former selectively elevated in CMS+ in direct proportion to CMS scores. The average OH-adduct concentration was comparable to that induced by maximal exercise in lowlanders following 2-hydroxypropyl-β-CD-assisted DEPMPO spin-trapping [46] at identical (final) concentrations to those employed herein, placing the magnitude of 'basal' oxidative stress to which the CMS+ patient is chronically exposed over their lifetime into clearer perspective.

In chiral nitrones such as DEPMPO or Me_2CyDEPMPO that form EPR distinguishable *cis*/*trans*-OH diastereoisomers upon trapping HO•, the *trans*/*cis* ratio determined under controlled conditions (e.g. at a given time after direct inhibition of HO-adduct formation) can differentiate between competing mechanisms that give rise to Me_2CyDEPMPO-OH. These include (*i*) bioreduction of primary Me_2CyDEPMPO-OOH by endogenous thiols or enzymes including reduced glutathione (GSH) and glutathione peroxidase (GPx), (*ii*) direct trapping of biologically relevant HO• by a metal ion-catalysed (e.g. Fe^{2+}) Fenton mechanism initiated by dismutation of primary $O_2^{\cdot-}$ to H_2O_2 (Eq. 2) and (*iii*) nucleophilic addition (NA) of water to the nitronyl function catalysed by metal ions such as Fe^{3+} (Forrester–Hepburn mechanism) that can be released during systemic OXNOS and subsequently reduced to Fe^{2+} by $O_2^{\cdot-}$ (Eq. 1) [22, 47, 48].

The *trans:cis* ratios obtained in CMS+ patients were more consistent with a Fenton

and/or NA mechanism (typical ratios of ~1.4 AU observed in vitro), since appreciably higher ratios (~3.0 AU) arise during GSH + GPx-induced reduction of primary OOH [22]. While this may argue against $O_2^{\cdot-}$ formation, it is conceivable that OOH-adducts may have initially formed, yet were rapidly reduced to OH-adducts before entry into the MeβCD inner cavity requisite for EPR detection. This is plausible given that the oxidative stress cascade is typically initiated by $O_2^{\cdot-}$ with HO• formed as a secondary species.

Detection of $A^{\cdot-}$, albeit in a random (sub) sample of CMS+ patients, suggests that 'free' iron was bioavailable with a catalytic efficiency comparable to Fe(III)-EDTA, lending further support to the proposed Fenton and/or NA mechanisms. This was complimented by detection of PBN-adducts assigned to secondary •OR formed downstream of Fe^{2+}-catalysed reductive decomposition of lipid hydroperoxides (LOOH) since equivalent hfcs have been observed in vitro following (Fe^{2+}-catalysed) auto-oxidation of cumene-OOH [3]. That the minor signal ascribed to Me_2CyDEPMPO-alkyl adducts were likely artefacts originating from the MeβCD structure potentially explains why further elevation was not observed in CMS+. In contrast, carbonylation was selectively elevated indicating that proteins are more vulnerable to OXNOS-mediated oxidative damage to amino acid side chains and protein backbone [49].

The complimentary examination of iron metabolites indicated that free iron in CMS+ did not arise as a result of iron exceeding transferrin binding capacity since TSAT, as indeed all associated metrics, were normal and comparable to healthy lowlander/CMS- participants. Intravascular hemolysis caused by mechanical stress associated with increased intrinsic blood viscosity [6] and/or oxidative damage to the RBC membrane

[50] is a plausible alternative. In support, a recent study documented an inverse relationship between free plasma haptoglobin and hematocrit in CMS+, suggesting that these patients are potentially exposed to lifelong hemolysis [51].

4.2. Dietary antioxidants

Only one study has previously estimated dietary intake in CMS+, albeit using a non-validated questionnaire limited to vitamins A, C and E. Despite indirect evidence for elevated lipid peroxidation in (Andean) CMS+, vitamin intake was comparable to healthy lowlander and CMS- controls [52]. In contrast, our validated, more comprehensive approach identified that intake of select antioxidant micronutrients including vitamins C and E, carotene, magnesium and retinol was generally lower in highlanders due to reduced F+V consumption.

Although the traditional Bolivian diet is predominantly based on foods of plant origin including potatoes and cereals, F+V have been subject to frequent price increases [53] that may have contributed to the lower consumption observed. However, why intake was further supressed in CMS+ remains unclear, especially in light of comparable SES. Indeed, vegetable and vitamin C intake were especially inadequate, falling below the minimum amount advised by UK [54] and Bolivian [55] Governments.

Our findings disagree with the latest Bolivian households' survey data [53] and first comprehensive review of dietary intake in Andean countries, indicating that vitamin C intake is generally sufficient in this population [56]. Inadequate intake may thus contribute, at least in part, to the lower systemic concentration of ascorbate (in combination with α- and β-carotene) previously documented in CMS+ [3]. This may further enhance vulnerability to OXNOS-mediated impairments in systemic vascular

endothelial function and structure (see 4.3) given that ascorbate is the primary water-soluble chain-breaking antioxidant required for targeted 'repair' of $O_2^{\cdot-}$, HO•, alkyl, peroxyl, •OR and tocopheroxyl radicals during chain propagation, the latter synergising regeneration of α-tocopherol, the primary fat-soluble chain-breaking antioxidant [57].

Equally, lower dietary intake of nitrate, primarily sourced through green, leafy vegetables with bioactivity (likely) further reduced due to overcooking [58] when added to traditional Bolivian 'sopas' (soups), may have also contributed to the lower plasma NO_2^- observed (4.2.). Clinically, inadequate F+V compounds OXNOS and increases corresponding risk of cardiovascular disease (CVD) and stroke [59], the primary causes of mortality in CMS+ patients who exhibit >3.6 fold higher CVD risk relative to healthy CMS- [60]. It has recently been identified that ≈5 daily servings daily of F+V confers the lowest risk of total and cause-specific mortality (albeit in lowlanders), with 2 (daily) servings for fruit and 3 for vegetables identified as the minimum required for risk reduction [59].

Clearly, the dietary behavior of CMS+ patients in the present study places them at higher CVD risk yet provides an opportunity for therapeutic intervention (pharmacological and/or dietary) in a bid to bolster endogenous antoxidant defences. Our findings provide a mechanistic basis justifying implementation of a prospective randomised trial to assess the impact of dietary manipulation on CMS+ given that OXNOS and corresponding hemodynamic risk factors may be at least, partially reversible. This may take the form of a randomised, controlled parallel-group community trial with CMS+ patients randomly assigned to either an interventional (encouraged to consume 5 daily servings of F+V consistent with aforementioned guidelines [59], also

incorporating transtheoretically-determined readiness for change combined with educational activities and problematising-dialogic pedagogy [61]) or control (maintenance of habitual dietary intake) group. We recommend a trial duration of 6 months given that this approach has been shown to augment circulating water and lipid-phase antioxidants (α-carotene, β-carotene, lutein, β-cryptoxanthin and ascorbic acid) and improve corresponding vascular funtion (reduction in systolic/diastolic blood pressure) [62].

4.3. Systemic vascular function and structure

In addition to direct scavenging of endothelial NO via diffusion-limited reactions with $O_2^{\cdot-}$, $RO^{\bullet}$ and $RC^{\bullet}$ [16], hemolysis-induced extravasation of cell-free Hb into plasma can further compound elimination via additional Fenton, NO dioxygenation [$Hb\text{-}Fe^{2+}(O_2)$ + $NO \rightarrow Hb\text{-}Fe^{3+}OONO^{\bullet}/NO_3^-$) and iron nitrosylation of deoxy-Hb [$Hb\text{-}Fe^{2+}$ + $NO \rightarrow Hb(NO)$] reactions [63]. These outcompete reaction with intra-erythrocytic Hb by ~1000-fold [64], reducing rates of *S*-nitrosothiol formation and/or deoxyHb-mediated reduction of NO_2^- to NO, stable (i.e. RBC-encapsulated) metabolites that conserve/transfer bioactivity within the hypoxic microcirculation. Indeed, hemolysis-induced NO scavenging and corresponding impairments in vascular endothelial function are common to (other) diseases characterised by increased RBC mass, including polycythemia vera and Chuvash polycythemia [65].

In the present study, plasma NO_2^- was generally lower in highlanders' blood and consistently associated with reduced systemic vascular endothelial function (FMD), elevated arterial stiffness (aPWV/AIx-75) and morphological impairment (elevated cIMT)

confirming our prior observations [3, 5]. However, that plasma NO_2^- was not further reduced in CMS+ despite more pronounced impairments in systemic vascular function and structure, suggests that vasculopathic complications cannot solely be ascribed to disordered NO metabolism (notwithstanding interpretive challenges associated with a small sample size, see 4.4. Experimental limitations). In support and contrary to prior observations [3, 5], GTN-induced dilation was also selectively attenuated in CMS+ albeit complicated by a tendency towards an elevated baseline diameter (arguably constraining further vasodilation), tentatively implying additional impairments in smooth muscle function and/or structure previously ascribed to direct vasculotoxic/constrictive effects of hypoxia-induced $O_2^{\cdot-}$ formation [66].

Intriguingly, aPWV widely considered the gold standard metric of aortic stiffness and independent predictor of coronary heart disease and stroke [67], provided the most robust differences and associations distinguishing vascular impairment in CMS+. While we cannot discount (aforementioned) statistical idiosyncrasies associated with a small sample size combined with differences in biomarker sensitivity/specificity, our findings tentatively suggest that elevated OXNOS may have selectively targeted (impaired) aortic stiffness over vascular endothelial function. Although speculative, this may be due to the fact that aortic stiffness is largely governed by structural degeneration of the scaffolding proteins, collagen and elastin, that are especially (if not perhaps more) vulnerable to mitochondrial ROS [68]. Figure 6 provides an overall schematic summarising the proposed molecular pathways underlying systemic OXINOS and corresponding link(s) to vasculopathic complications of CMS (including novel contributions in the present study), extending our previously published findings [3, 7].

4.4. Experimental limitations

Several limitations warrant careful consideration to provide a more balanced perspective to the present findings. All findings were based exclusively on cross-sectional comparisons and correlational analyses in the absence of mediation analysis, warranting future interventional approaches to better define a causal role for OXNOS as mediators of vascular dysfunction and/or CMS disease process (see 4.5 Conclusions).

We also acknowledge the interpretive limitations associated with a relatively small sample size and associated loss of statistical power; including caveats associated with Type II and M errors [69], that for select variables, in particular FMD, AIx-75, NO_2^- and vitamin E, limited our ability to detect post-hoc differences between CMS+ and CMS-. In terms of (absolute %) FMD values, we (retrospectively) observed an effect size of 1.067 and corresponding power of 0.998 ($\alpha = 0.05$), having adhered strictly to established guidelines that have been shown to reduce variability [70], indicating that our study was well powered to detect a treatment effect. However, our conservative approach (Bonferroni adjustments to control for false positives), combined with recent evidence documenting CVs of 16.6% and 14.2% and intra-class correlation coefficients of 0.528 and 0.714 for intra- and inter-session brachial FMD test-retests respectively [71] suggests that this technique is at best, only 'moderately' reliable, that warrants consideration during future research.

We also recognise the need to exercise caution when attempting to unequivocally assign spin-adducts to specific free radical species/mechanisms; while these can be better approached in vitro using 'stopped generators', this was not possible ex vivo

given that continuous free radical formation persists over the course of blood sampling, notwithstanding the potential for artefactual $O_2^{\cdot-}$/HO• generation during the course of incubation and sample processing. Indeed, this is a universal challenge when attempting to detect 'any' reactive metabolite ex vivo in the human circulation (i.e. not just free radicals) that are formed clearly downstream of the primary reaction pathway that we assume reflects dynamic events in vivo. Recently, we pretreated PBN trapped blood with ethylgallimidate in an attempt to inhibit (neutrophil) NADPH oxidase activation as originally recommended [11], although initial findings indicated this had little to no measurable effect in terms of PBN-OR formation (DM Bailey, unpublished observations). Follow-up quality control approaches are warranted given the reactivity of free radicals and complexity of blood as a biological matrix. Future studies aimed at elucidating the targets of the generated $O_2^{\cdot-}$ and HO• are also warranted, including 'proteomics' to explore the thiol redox proteome [72] and 'immuno-spin trapping' that combines the specificity of spin trapping with improved sensitivity of immunological techniques with nitrone adducts that can be detected by mass spectrometry, NMR or immunochemistry using anti-DMPO nitrone antibodies [73, 74].

Due to logistics constraints, lowlander controls were recruited from the UK and not Bolivia. Expected differences in socio-cultural influences (e.g., access to healthcare, social/family structure) likely complicated our ability to accurately distinguish whether observed differences were due to HA residence or CMS per se. Likewise, future researchers need to consider investigating females, especially those who are postmenopausal, given that this is a risk factor for CMS [75]. Furthermore, catalytic iron detection and general assessment of iron metabolism were confined to either a select

(sub) sample of CMS+ patients or entirely separate group respectively, as ‘follow-ups’ upon successful detection of Me_2CyDEPMPO-OH adducts. Complimentary assays of intravascular hemolysis specifically cell-free Hb, hemopexin and haptoglobin are also encouraged in future studies to complement the present findings.

Finally, while select aspects of elevated OXNOS biomarkers and systemic vascular dysfunction have previously been reported in CMS+ [3, 7], the new data generated by the present study (Figure 6) further extends our mechanistic understanding of the systemic OXNOS pathway.

4.5. Conclusions

In conclusion, the present study suggests that elevated systemic OXNOS and associated vasculopathic complications in CMS+ may be the consequence of iron-induced oxidative catalysis that may have a Fenton/NA/hemolytic basis. Future studies need to further differentiate these mechanisms and consider related pharmacological/dietary approaches that selectively target the OXNOS pathway including iron chelation (e.g. desferroxamine) to constrain iron-mediated oxidative catalysis. Equally, prospective randomized trials and/or public health interventions aimed at encouraging more F+V consumption will help address dietary antioxidant deficiency, reduce vulnerability to OXNOS and improve clinical outcome.

Acknowledgements

We thank Mrs Catherine Romero and staff of the Instituto Boliviano de Biologia de Altura (La Paz, Bolivia) for technical support. ADInstruments provided exceptional

technical input/support during the period of data logging. We also thank Professor Martina Muckenthaler (University of Heidelberg, Heidelberg, Germany) for specialist input relating to iron metabolism.

Competing interests

The authors declare that they have no competing interests.

Funding

This work was supported by a Royal Society Wolfson Research Fellowship (#WM170007) and grants from the Higher Education Funding Council for Wales (DMB), Swiss National Science Foundation, Cloëtta Foundation, Eagle Foundation, Leenaards Foundation and Placide Nicod Foundation (US and CS).

Author contributions

DMB, US and CS obtained funding, conceived and designed the research. DMB, MC, TF, JVB, BS, CJM, RS, SFR, DC, ER, LP, CSS, CMJ, MV, FV, AR, SP, US and CS contributed to data collection and/or analysis. DMB, MC, TF, AR, SP, US and CS interpreted the results of the experiments. DMB drafted the first draft manuscript and revisions thereof with input from MC, US and CS. DMB, MC, TF, JVB, BS, CJM, RS, SFR, DC, ER, LP, CSS, CMJ, MV, FV, AR, SP, US and CS edited and revised the manuscript(s) and approved the final version submitted for publication.

Appendix A. Supplementary material

Supplementary data associated with this article can be found in the online version.

REFERENCES

[1] F. Leon-Velarde, M. Maggiorini, J.T. Reeves, A. Aldashev, I. Asmus, L. Bernardi, R.L. Ge, P. Hackett, T. Kobayashi, L.G. Moore, D. Penaloza, J.P. Richalet, R. Roach, T. Wu, E. Vargas, G. Zubieta-Castillo, G. Zubieta-Calleja, Consensus statement on chronic and subacute high altitude diseases, High altitude medicine & biology 6(2) (2005) 147-57.

[2] D. Penaloza, J. Arias-Stella, The heart and pulmonary circulation at high altitudes: healthy highlanders and chronic mountain sickness, Circulation 115(9) (2007) 1132-46.

[3] D.M. Bailey, S.F. Rimoldi, E. Rexhaj, L. Pratali, C. Salinas Salmon, M. Villena, J. McEneny, I.S. Young, P. Nicod, Y. Allemann, U. Scherrer, C. Sartori, Oxidative-nitrosative stress and systemic vascular function in highlanders with and without exaggerated hypoxemia, Chest 143(2) (2013) 444-451.

[4] E. Rexhaj, S.F. Rimoldi, L. Pratali, R. Brenner, D. Andries, R. Soria, C. Salinas, M. Villena, C. Romero, Y. Allemann, A. Lovis, R. Heinzer, C. Sartori, U. Scherrer, Sleep-Disordered Breathing and Vascular Function in Patients With Chronic Mountain Sickness and Healthy High-Altitude Dwellers, Chest 149(4) (2016) 991-8.

[5] S.F. Rimoldi, E. Rexhaj, L. Pratali, D.M. Bailey, D. Hutter, F. Faita, C. Salinas Salmon, M. Villena, P. Nicod, Y. Allemann, U. Scherrer, C. Sartori, Systemic vascular dysfunction in patients with chronic mountain sickness, Chest 141(1) (2012) 139-46.

[6] J.C. Tremblay, R.L. Hoiland, C.A. Howe, G.B. Coombs, G.A. Vizcardo-Galindo, R.J. Figueroa-Mujica, D. Bermudez, T.D. Gibbons, B.S. Stacey, D.M. Bailey, M.M. Tymko, D.B. MacLeod, C. Gasho, F.C. Villafuerte, K.E. Pyke, P.N. Ainslie, Global REACH 2018:

High blood viscosity and hemoglobin concentration contribute to reduced flow-mediated dilation in high-altitude excessive erythrocytosis, Hypertension 73(6) (2019) 1327-1335.

[7] D.M. Bailey, J.V. Brugniaux, T. Filipponi, C.J. Marley, B. Stacey, R. Soria, S.F. Rimoldi, D. Cerny, E. Rexhaj, L. Pratali, C.S. Salmon, C. Murillo Jauregui, M. Villena, J.D. Smirl, S. Ogoh, S. Pietri, U. Scherrer, C. Sartori, Exaggerated systemic oxidative-inflammatory-nitrosative stress in chronic mountain sickness is associated with cognitive decline and depression, The Journal of physiology 597(2) (2019) 611-629.

[8] K.A. Smith, G.B. Waypa, P.T. Schumacker, Redox signaling during hypoxia in mammalian cells, Redox biology 13 (2017) 228-234.

[9] P. Hernansanz-Agustin, C. Choya-Foces, S. Carregal-Romero, E. Ramos, T. Oliva, T. Villa-Pina, L. Moreno, A. Izquierdo-Alvarez, J.D. Cabrera-Garcia, A. Cortes, A.V. Lechuga-Vieco, P. Jadiya, E. Navarro, E. Parada, A. Palomino-Antolin, D. Tello, R. Acin-Perez, J.C. Rodriguez-Aguilera, P. Navas, A. Cogolludo, I. Lopez-Montero, A. Martinez-Del-Pozo, J. Egea, M.G. Lopez, J.W. Elrod, J. Ruiz-Cabello, A. Bogdanova, J.A. Enriquez, A. Martinez-Ruiz, Na(+) controls hypoxic signalling by the mitochondrial respiratory chain, Nature 586(7828) (2020) 287-291.

[10] M.P. Murphy, How mitochondria produce reactive oxygen species, The Biochemical journal 417(1) (2009) 1-13.

[11] D.M. Bailey, S. Taudorf, R.M.G. Berg, C. Lundby, J. McEneny, I.S. Young, K.A. Evans, P.E. James, A. Shore, D.A. Hullin, J.M. McCord, B.K. Pedersen, K. Moller, Increased cerebral output of free radicals during hypoxia: implications for acute mountain sickness?, American Journal of Physiology (Regulatory, Integrative and Comparative Physiology) 297(5) (2009) R1283-1292.

[12] D.M. Bailey, P. Rasmussen, K.A. Evans, A.M. Bohm, M. Zaar, H.B. Nielsen, P. Brassard, N.B. Nordsborg, P.H. Homann, P.B. Raven, J. McEneny, I.S. Young, J.M. McCord, N.H. Secher, Hypoxia compounds exercise-induced free radical formation in humans; partitioning contributions from the cerebral and femoral circulation, Free Radical Biology & Medicine

124 (2018) 104-113.

[13] T. Munzel, A. Daiber, V. Ullrich, A. Mulsch, Vascular consequences of endothelial nitric oxide synthase uncoupling for the activity and expression of the soluble guanylyl cyclase and the cGMP-dependent protein kinase, Arteriosclerosis, thrombosis, and vascular biology 25(8) (2005) 1551-7.

[14] P. Hernansanz-Agustin, A. Izquierdo-Alvarez, F.J. Sanchez-Gomez, E. Ramos, T. Villa-Pina, S. Lamas, A. Bogdanova, A. Martinez-Ruiz, Acute hypoxia produces a superoxide burst in cells, Free radical biology & medicine 71 (2014) 146-156.

[15] G.R. Buettner, The pecking order of free radicals and antioxidants: lipid peroxidation, *α*-tocopherol, and ascorbate., Archives of biochemistry and biophysics 300(2) (1993) 535-543.

[16] T. Nauser, W.H. Koppenol, The rate constant of the reaction of superoxide with nitrogen monoxide: approaching the diffusion limit., Journal of Physical Chemistry A 106 (2002) 4084-4086.

[17] I. Fridovich, The biology of oxygen radicals, Science 201(4359) (1978) 875-80.

[18] E. von Elm, D.G. Altman, M. Egger, S.J. Pocock, P.C. Gotzsche, J.P. Vandenbroucke, S. Initiative, The Strengthening the Reporting of Observational Studies

in Epidemiology (STROBE) Statement: guidelines for reporting observational studies, International Journal of Surgery 12(12) (2014) 1495-9.

[19] D.M. Bailey, C.J. Marley, J.V. Brugniaux, D. Hodson, K.J. New, S. Ogoh, P.N. Ainslie, Elevated aerobic fitness sustained throughout the adult lifespan is associated with improved cerebral hemodynamics, Stroke 44(11) (2013) 3235-8.

[20] K. Fujishiro, J. Xu, F. Gong, What does “occupation” represent as an indicator of socioeconomic status?: Exploring occupational prestige and health, Social Science & Medicine 71 (2010) 2100-2107.

[21] K.H. Wesseling, J.R. Jansen, J.J. Settels, J.J. Schreuder, Computation of aortic flow from pressure in humans using a nonlinear, three-element model, Journal of applied physiology 74(5) (1993) 2566-73.

[22] G. Gosset, J.L. Clément, M. Culcasi, A. Rockenbauer, S. Pietri, CyDEPMPOs: a class of stable cyclic DEPMPO derivatives with improved properties as mechanistic markers of stereoselective hydroxyl radical adduct formation in biological systems, Bioorganic and Medicinal Chemistry 19(7) (2011) 2218-30.

[23] H. Karoui, A. Rockenbauer, S. Pietri, P. Tordo, Spin trapping of superoxide in the presence of beta-cyclodextrins, Chemical Communications (Cambridge) (24) (2002) 3030-1.

[24] K. Abbas, M. Hardy, F. Poulhes, H. Karoui, P. Tordo, O. Ouari, F. Peyrot, Detection of superoxide production in stimulated and unstimulated living cells using new cyclic nitrone spin traps, Free radical biology & medicine 71 (2014) 281-290.

[25] A. Rockenbauer, L. Korecz, Automatic computer simulation of ESR spectra. , Applied Magnetic Resonance 10 (1996) 29-43.

[26] G. Buettner, W. Chamulitrat, The catalytic activity of iron in synovial fluid as monitored by the ascorbate free radical., Free radical biology & medicine 8(1) (1990) 55-6.

[27] A. Adamski, T. Spalek, A. Sojka, Application of EPR spectroscopy for elucidation of vanadium speciation in VOx/ZrO_2 catalysts subject to redox treatment Research on Chemical Intermediates 29 (2003) 793-804.

[28] J.P. Vuilleumier, E. Keck, Fluorimetric assay of vitamin C in biological materials using a centrifugal analyser with fluorescence attachment., Journal of Micronutritional Analysis 5 (1993) 25-34.

[29] P. Stocker, M. Cassien, N. Vidal, S. Thétiot-Laurent, S. Pietri, A fluorescent homogeneous assay for myeloperoxidase measurement in biological samples. A positive correlation between myeloperoxidase-generated HOCl level and oxidative status in STZ-diabetic rats, Talanta 170 (2017) 119-127.

[30] D.M. Bailey, P. Rasmussen, M. Overgaard, K.A. Evans, A.M. Bohm, T. Seifert, P. Brassard, M. Zaar, H.B. Nielsen, P.B. Raven, N.H. Secher, Nitrite and *S*-Nitrosohemoglobin exchange across the human cerebral and femoral circulation: relationship to basal and exercise blood flow responses to hypoxia, Circulation 135(2) (2017) 166-176.

[31] I. Kasvosve, J. Delanghe, Total iron binding capacity and transferrin concentration in the assessment of iron status, Clin Chem Lab Med 40(10) (2002) 1014-8.

[32] R.S. Gibson, Principles of nutritional assessment, Oxford University Press, New York, USA, 2005.

[33] R.S. Gibson, U.R. Charrondiere, W. Bell, Measurement Errors in Dietary Assessment Using Self-Reported 24-Hour Recalls in Low-Income Countries and Strategies for Their Prevention, Advances in Nutrition 8 (2017) 980-991.

[34] F.E. Thompson, A.F. Subar, Dietary Assessment Methodology, in: A.M. Coulston, C.J. Boushey, M.G. Ferruzzi (Eds.), Nutrition in the prevention and treatment of disease, Academic Press, London, UK, 2017, pp. 5-48.

[35] P.Y. Jayet, S.F. Rimoldi, T. Stuber, C.S. Salmon, D. Hutter, E. Rexhaj, S. Thalmann, M. Schwab, P. Turini, C. Sartori-Cucchia, P. Nicod, M. Villena, Y. Allemann, U. Scherrer, C. Sartori, Pulmonary and systemic vascular dysfunction in young offspring of mothers with preeclampsia, Circulation 122(5) 488-94.

[36] J. Deanfield, A. Donald, C. Ferri, C. Giannattasio, J. Halcox, S. Halligan, A. Lerman, G. Mancia, J.J. Oliver, A.C. Pessina, D. Rizzoni, G.P. Rossi, A. Salvetti, E.L. Schiffrin, S. Taddei, D.J. Webb, Endothelial function and dysfunction. Part I: Methodological issues for assessment in the different vascular beds: a statement by the Working Group on Endothelin and Endothelial Factors of the European Society of Hypertension, Journal of Hypertension 23(1) (2005) 7-17.

[37] V. Gemignani, F. Faita, L. Ghiadoni, E. Poggianti, M. Demi, A system for real-time measurement of the brachial artery diameter in B-mode ultrasound images, IEEE Transactions in Medical Imaging 26(3) (2007) 393-404.

[38] G. Atkinson, A.M. Batterham, The percentage flow-mediated dilation index: a large-sample investigation of its appropriateness, potential for bias and causal nexus in vascular medicine, Vasc Med 18(6) (2013) 354-65.

[39] S. Laurent, J. Cockcroft, L. Van Bortel, P. Boutouyrie, C. Giannattasio, D. Hayoz, B. Pannier, C. Vlachopoulos, I. Wilkinson, H. Struijker-Boudier, Expert consensus document on arterial stiffness: methodological issues and clinical applications, Eur Heart J 27(21) (2006) 2588-605.

[40] R. Asmar, A. Benetos, J. Topouchian, P. Laurent, B. Pannier, A.M. Brisac, R. Target, B.I. Levy, Assessment of arterial distensibility by automatic pulse wave velocity measurement. Validation and clinical application studies, Hypertension 26(3) (1995) 485-90.

[41] M. O'Rourke, Arterial stiffness, systolic blood pressure, and logical treatment of arterial hypertension, Hypertension (15) (1990) 339-347.

[42] I.B. Wilkinson, H. MacCallum, L. Flint, J.R. Cockcroft, D.E. Newby, D.J. Webb, The influence of heart rate on augmentation index and central arterial pressure in humans, Journal of Physiology 525 Pt 1 (2000) 263-70.

[43] J.H. Stein, C.E. Korcarz, R.T. Hurst, E. Lonn, C.B. Kendall, E.R. Mohler, S.S. Najjar, C.M. Rembold, W.S. Post, Use of carotid ultrasound to identify subclinical vascular disease and evaluate cardiovascular disease risk: a consensus statement from the American Society of Echocardiography Carotid Intima-Media Thickness Task Force. Endorsed by the Society for Vascular Medicine, Journal of the American Society of Echocardiography 21(2) (2008) 93-111.

[44] P.J. Touboul, M.G. Hennerici, S. Meairs, H. Adams, P. Amarenco, N. Bornstein, L. Csiba, M. Desvarieux, S. Ebrahim, M. Fatar, R. Hernandez Hernandez, M. Jaff, S. Kownator, P. Prati, T. Rundek, M. Sitzer, U. Schminke, J.C. Tardif, A. Taylor, E. Vicaut, K.S. Woo, F. Zannad, M. Zureik, Mannheim carotid intima-media thickness consensus

(2004-2006). An update on behalf of the Advisory Board of the 3rd and 4th Watching the Risk Symposium, 13th and 15th European Stroke Conferences, Mannheim, Germany, 2004, and Brussels, Belgium, 2006, Cerebrovascular Disorders 23(1) (2007) 75-80.

[45] J.N. Cobley, M.L. Fiorello, D.M. Bailey, 13 reasons why the brain is susceptible to oxidative stress, Redox biology 15 (2018) 490-503.

[46] D.M. Bailey, K.A. Evans, J. McEneny, I.S. Young, D.A. Hullin, P.E. James, S. Ogoh, P.N. Ainslie, C. Lucchesi, A. Rockenbauer, M. Culcasi, S. Pietri, Exercise-induced oxidative-nitrosative stress is associated with impaired dynamic cerebral autoregulation and blood-brain barrier leakage, Experimental physiology 96(11) (2011) 1196-207.

[47] C. Fréjaville, H. Karoui, B. Tuccio, F. Le Moigne, M. Culcasi, S. Pietri, R. Lauricella, P. Tordo, 5-(Diethoxyphosphoryl)-5-methyl-1-pyrroline *N*-oxide: a new efficient phosphorylated nitrone for the in vitro and in vivo spin trapping of oxygen-centered radicals, Journal of medicinal chemistry 38(2) (1995) 258-65.

[48] M. Culcasi, A. Rockenbauer, A. Mercier, J.L. Clément, S. Pietri, The line asymmetry of electron spin resonance spectra as a tool to determine the cis:trans ratio for spin-trapping adducts of chiral pyrrolines N-oxides: the mechanism of formation of hydroxyl radical adducts of EMPO, DEPMPO, and DIPPMPO in the ischemic-reperfused rat liver, Free Radical Biology and Medicine 40(9) (2006) 1524-38.

[49] E.R. Stadtman, R.L. Levine, Free radical-mediated oxidation of free amino acids and amino acid residues in proteins, Amino Acids 25(3-4) (2003) 207-18.

[50] O.G. Luneva, S.V. Sidorenko, O.O. Ponomarchuk, A.M. Tverskoy, A.A. Cherkashin, O.V. Rodnenkov, N.V. Alekseeva, L.I. Deev, G.V. Maksimov, R. Grygorczyk, S.N. Orlov, Deoxygenation Affects Composition of Membrane-Bound Proteins in Human Erythrocytes, Cell Physiol Biochem 39(1) (2016) 81-8.

[51] J.L. Macarlupu, G. Vizcardo-Galindo, R. Figueroa-Mujica, N. Voituron, J.P. Richalet, F.C. Villafuerte, Sub-maximal aerobic exercise training reduces haematocrit and ameliorates symptoms in Andean highlanders with chronic mountain sickness, Experimental physiology (2021).

[52] J.A. Jefferson, J. Simoni, E. Escudero, M.E. Hurtado, E.R. Swenson, D.E. Wesson, G.F. Schreiner, R.B. Schoene, R.J. Johnson, A. Hurtado, Increased oxidative stress following acute and chronic high altitude exposure, High altitude medicine & biology 5(1) (2004) 61-9.

[53] F.J. Pérez-Cueto, A. Naska, J. Monterrey, M. Almanza-Lopez, A. Trichopoulou, P. Kolsteren, Monitoring food and nutrient availability in a nationally representative sample of Bolivian households, Br J Nutr 95(3) (2006) 555-67.

[54] D.o. Health, Dietary reference values for food and nutrients for the United Kingdom. Report of the Panel on Dietary Reference Values of the Committee on Medical Aspects of Food Policy., London, UK, 1991.

[55] M.d.S.d. Bolivia, Ministerio de Salud. Bases técnicas de las guías alimentarias para la población Boliviana, La Paz, Bolivia, 2014, pp. 1-100.

[56] P.R. Berti, C. Fallu, Y. Cruz Agudo, A systematic review of the nutritional adequacy of the diet in the Central Andes, Rev Panam Salud Publica 36(5) (2014) 314-23.

[57] M. Sharma, G. Buettner, Interaction of vitamin C and vitamin E during free radical stress in plasma: an ESR study., Free Radicals in Biology and Medicine 14(6) (1993) 649-53.

[58] A. Ahluwalia, M. Gladwin, G.D. Coleman, N. Hord, G. Howard, D.B. Kim-Shapiro, M. Lajous, F.J. Larsen, D.J. Lefer, L.A. McClure, B.T. Nolan, R. Pluta, A. Schechter, C.Y. Wang, M.H. Ward, J.L. Harman, Dietary Nitrate and the Epidemiology of Cardiovascular Disease: Report From a National Heart, Lung, and Blood Institute Workshop, J Am Heart Assoc 5(7) (2016).

[59] D.D. Wang, Y. Li, S.N. Bhupathiraju, B.A. Rosner, Q. Sun, E.L. Giovannucci, E.B. Rimm, J.E. Manson, W.C. Willett, M.J. Stampfer, F.B. Hu, Fruit and Vegetable Intake and Mortality: Results From 2 Prospective Cohort Studies of US Men and Women and a Meta-Analysis of 26 Cohort Studies, Circulation 143(17) (2021) 1642-1654.

[60] N. Corante, C. Anza-Ramirez, R. Figueroa-Mujica, J.L. Macarlupu, G. Vizcardo-Galindo, G. Bilo, G. Parati, J.L. Gamboa, F. Leon-Velarde, F.C. Villafuerte, Excessive Erythrocytosis and Cardiovascular Risk in Andean Highlanders, High Alt Med Biol 19(3) (2018) 221-231.

[61] M.C. Menezes, R.D. Mendonca, N.L. Ferreira, L.M.F. Guimaraes, A.C.S. Lopes, Promoting fruit and vegetable consumption: Methodological protocol of a randomized controlled community trial, Contemp Clin Trials Commun 10 (2018) 131-136.

[62] J.H. John, S. Ziebland, P. Yudkin, L.S. Roe, H.A. Neil, F. Oxford, G. Vegetable Study, Effects of fruit and vegetable consumption on plasma antioxidant concentrations and blood pressure: a randomised controlled trial, Lancet 359(9322) (2002) 1969-74.

[63] G.J. Kato, M.H. Steinberg, M.T. Gladwin, Intravascular hemolysis and the pathophysiology of sickle cell disease, J Clin Invest 127(3) (2017) 750-760.

[64] C.D. Reiter, X. Wang, J.E. Tanus-Santos, N. Hogg, R.O. Cannon, 3rd, A.N. Schechter, M.T. Gladwin, Cell-free hemoglobin limits nitric oxide bioavailability in sickle-cell disease, Nat Med 8(12) (2002) 1383-9.

[65] M.T. Gladwin, R.P. Patel, The role of red blood cells and hemoglobin-nitric oxide interactions on blood flow, Am J Respir Cell Mol Biol 38(2) (2008) 125-6.

[66] N.C. Lewis, D.M. Bailey, G.R. Dumanoir, L. Messinger, S.J. Lucas, J.D. Cotter, J. Donnelly, J. McEneny, I.S. Young, M. Stembridge, K.R. Burgess, A.S. Basnet, P.N. Ainslie, Conduit artery structure and function in lowlanders and native highlanders: relationships with oxidative stress and role of sympathoexcitation, The Journal of physiology 592(5) (2014) 1009-24.

[67] G.F. Mitchell, S.J. Hwang, R.S. Vasan, M.G. Larson, M.J. Pencina, N.M. Hamburg, J.A. Vita, D. Levy, E.J. Benjamin, Arterial stiffness and cardiovascular events: the Framingham Heart Study, Circulation 121(4) (2010) 505-11.

[68] R.H. Zhou, A.E. Vendrov, I. Tchivilev, X.L. Niu, K.C. Molnar, M. Rojas, J.D. Carter, H. Tong, G.A. Stouffer, N.R. Madamanchi, M.S. Runge, Mitochondrial oxidative stress in aortic stiffening with age: the role of smooth muscle cell function, Arteriosclerosis, thrombosis, and vascular biology 32(3) (2012) 745-55.

[69] A. Gelman, J. Carlin, Beyond Power Calculations: Assessing Type S (Sign) and Type M (Magnitude) Errors, Perspect Psychol Sci 9(6) (2014) 641-51.

[70] A. Greyling, A.C. van Mil, P.L. Zock, D.J. Green, L. Ghiadoni, D.H. Thijssen, T.I.W.G.o.F.M. Dilation, Adherence to guidelines strongly improves reproducibility of brachial artery flow-mediated dilation, Atherosclerosis 248 (2016) 196-202.

[71] R. Kimble, K.M. Keane, J.K. Lodge, G. Howatson, Methodological Considerations for a Vascular Function Test Battery, International journal of sports medicine 40(9) (2019) 601-608.

[72] J. Yang, K.S. Carroll, D.C. Liebler, The Expanding Landscape of the Thiol Redox Proteome, Mol Cell Proteomics 15(1) (2016) 1-11.

[73] R.P. Mason, Using anti-5,5-dimethyl-1-pyrroline N-oxide (anti-DMPO) to detect protein radicals in time and space with immuno-spin trapping, Free radical biology & medicine 36(10) (2004) 1214-23.

[74] R.P. Mason, D. Ganini, Immuno-spin trapping of macromolecules free radicals in vitro and in vivo - One stop shopping for free radical detection, Free radical biology & medicine 131 (2019) 318-331.

[75] F.C. Villafuerte, N. Corante, Chronic Mountain Sickness: Clinical Aspects, Etiology, Management, and Treatment, High altitude medicine & biology 17(2) (2016) 61-9.

LEGENDS

Fig. 1. Experimental design

NO, nitric oxide; $O_2^{\cdot-}$ superoxide anion; HO•, hydroxyl radical; CMS-/CMS+, highlanders without/with chronic mountain sickness (CMS). Red text highlights new measurements reported by the present study that compliment our previously published findings [3, 7].

Fig. 2. Cyclodextrin-assisted in vitro and ex vivo spin-trapping with Me_2CyDEPMPO and protein carbonyl formation in highlanders' blood

A. Chemical structure of 2-methyl-2-(5,5-dimethyl-2-oxo-1,3,2-dioxaphosphinan-2-yl)-3,4-dihydro-2H-pyrrole 1-oxide (Me_2CyDEPMPO) and formation of *trans*/*cis* diastereoisomers in the spin trapping of HO• and alkyl radicals. Inset: Structure of DEPMPO. B. Typical EPR signals at room temperature in the blood of CMS- vs. CMS+ highlanders. Immediately after drawing, samples were supplemented with Me_2CyDEPMPO (0.1 M) and MeβCD (80 mM) before being quickly frozen. Best fits yielded mixtures of *trans/cis* diastereoisomeric OH and alkyl adducts with hfcs (in G): CMS-: *trans*-OH: a_N = 13.87, a_P = 48.76, and $a_H^{ß}$ = 12.18 G; *cis*-OH: a_N = 14.23, a_P = 50.20 and $a_H^{ß}$ = 13.53 G; alkyl: a_N = 15.97, a_P = 47.92 and $a_H^{ß}$ = 22.43; CMS+: *trans*-OH: a_N = 13.70, a_P = 48.53 and $a_H^{ß}$ = 12.45 G; *cis*-OH: a_N = 14.15, a_P = 50.35 and $a_H^{ß}$ = 14.57 G; alkyl: a_N = 14.33, a_P = 50.34 and $a_H^{ß}$ = 20.43. Relative intensities are highlighted and the low-field lines of alkyl and OH adducts are visualised by the grey and black arrows, respectively. C. Spin adducts intensities (mean ± SD) in CMS- (n = 10) vs. CMS+ (n = 10) highlanders, with no adducts detected in lowlander blood. D. Basal protein carbonyls (mean ± SD) in CMS- (n = 10) vs. CMS+ (n = 10) highlanders.

Figure 3. EPR studies of catalytic iron and PBN spin adducts

A. Changes in $A^{\bullet-}$ concentration following ex vivo addition of DFX (500 µM) and Fe(III)-EDTA (10 µM) to blood obtained from CMS+ highlanders. Values are mean ± SD (n = 5) and expressed relative to ambient ascorbate concentration. B. Formation of alkoxyl radical ($RO^{\bullet}$) PBN spin adduct (PBN-OR). C. Typical PBN-OR EPR signals (a_N = 13.59 G and a_H^{β} = 1.85 G) observed in blood from a CMS+ patient. Inset: Typical baseline $A^{\bullet-}$ EPR doublet and structure of $A^{\bullet-}$ showing main coupling hydrogen (in bold).

Figure 4. Nitric oxide metabolites

Values are mean ± SD (n = 10 per group); NO_2^-, nitrite; RSNO, *S*-Nitrosothiols. Inset top right highlights typical (raw) composite signals observed in a single participant before (NO_2^- + RSNO) and after (RSNO, please see Methods) sulphanilamide incubation.

Figure 5. Relationships observed between free radical metabolism and systemic vascular function.

Me_2CyDEPMPO, 2-methyl-2-(5,5-dimethyl-2-oxo-1,3,2-dioxaphosphinan-2-yl)-3,4-dihydro-2H-pyrrole 1-oxide; OH, hydroxyl; FMD, flow-mediated dilation; PWV, pulse wave velocity; AIx-75, augmentation index normalised to heart rate of 75 b/min; CMS-/CMS+, highlanders without/with chronic mountain sickness (CMS). Note that only significant (i.e., $P < 0.05$) correlations are included.

Figure 6.

Summary schematic of the molecular pathways and link(s) to systemic vascular function/structural impairments in chronic mountain sickness.

I. Proposed stimuli underlying systemic activation of the oxidative nitrosative stress (OXNOS) pathway. II. Proposed OXNOS pathway highlighting free radical sources, mechanisms of formation and corresponding targets. Intravascular (mitochondrial/extra-mitochondrial) superoxide ($O_2^{\cdot-}$) and corresponding reductive formation of Fe^{2+} (ferrous iron) can catalyse Fenton/nucleophilic addition/hemolysis-induced generation of hydroxyl (HO•) and other secondary lipid-derived alkoxyl/alkyl radicals ($LO^{\bullet}$/$LC^{\bullet}$). These species are thermodynamically capable of causing oxidative damage to proteins including red blood cells and reacting directly with nitric oxide (NO) reducing bioavailability for smooth-muscle cells. Lifelong exposure to iron-catalysed systemic OXNOS, compounded by a dietary deficiency of antioxidant micronutrients, likely contributes to the vasculopathic complications and increased morbidity/mortality observed in CMS. Note those variables highlighted in red (filled boxes or text) indicate additional advances reported by the present study that compliment our previously published findings, providing additional mechanistic insight into the systemic OXNOS pathway [3, 7]. PaO_2, arterial partial pressure of oxygen; SaO_2, arterial oxyhemoglobin saturation; F + V, fruit and vegetables; $O_2^{\cdot-}$ superoxide anion; Fe^{3+}, ferric iron; H_2O_2, hydrogen peroxide; Me_2CyDEPMPO-OH, 2-methyl-2-(5,5-dimethyl-2-oxo-1,3,2-dioxaphosphinan-2-yl)-3,4-dihydro-2H-pyrrole 1-oxide-hydroxyl adduct; LOOH, lipid hydroperoxides; $LOO^{\bullet}$, lipid peroxyl radical; $ONOO^-$, peroxynitrite; Hb-$Fe^{2+}(O_2)$, ferrous oxyhemoglobin; Hb-Fe^{3+}, methemoglobin; NO_3^-, nitrate, Hb(NO), iron-

nitrosylhemoglobin; GTN-FMD, glyceryl trinitrate-stimulated FMD (endothelium-independent), flow-mediated dilatation (endothelium-dependent); aPWV, aortic pulse wave velocity; cIMT, carotid intima-media thickness.

Table 1. Demographics

Group:	**Lowlanders**	**Highlanders**		***P* values**		
Subgroup:	**Controls (n = 10)**	**CMS- (n = 10)**	**CMS+ (n = 10)**	**CMS- *vs*. Controls**	**CMS+ *vs*. Controls**	**CMS+ *vs*. CMS-**
Clinical						
Age (y)	57 ± 5	55 ± 8	56 ± 9	0.116 (between groups)		
Hb (g/dL)	14.0 ± 0.9	17.0 ± 1.0	20.3 ± 2.2	<0.001	<0.001	<0.001
Hct (%)	44 ± 3	52 ± 4	62 ± 7	0.003	<0.001	<0.001
SaO_2 (%)	97 ± 0	90 ± 6	88 ± 4	0.004	<0.001	0.443
caO_2 (mg/dL)	18.9 ± 1.2	21.3 ± 1.6	24.7 ± 3.0	0.044	<0.001	0.004
CMS score (points)	0 ± 0	1 ± 2	6 ± 4	0.677	<0.001	<0.001
Anthropometrics						
Mass (kg)	75.2 ± 9.3	71.8 ± 7.0	79.1 ± 11.9	0.256 (between groups)		
Stature (m)	1.75 ± 0.07	1.63 ± 0.03	1.61 ± 0.05	<0.001	<0.001	1.000
BMI (kg/m^2)	25 ± 3	27 ± 3	29 ± 4	0.349	0.022	0.629
Socioeconomic status						
Secondary educated (n/%)	6/60	6/60	8/80	0.549 (between groups)		
University educated (n/%)	4/40	4/40	2/20	0.549 (between groups)		
Occupational prestige (points)	50 ± 15	53 ± 17	41 ± 10	0.156 (between groups)		
Cardiopulmonary function						
PET_{O2} (mmHg)	106 ± 4	55 ± 3	53 ± 4	<0.001	<0.001	0.959
PET_{CO2} (mmHg)	41 ± 3	33 ± 5	34 ± 3	<0.001	0.001	1.000
SBP (mmHg)	131 ± 10	119 ± 20	135 ± 19	0.096 (between groups)		
DBP (mmHg)	78 ± 6	61 ± 8	69 ± 9	<0.001	0.066	0.108
MAP (mmHg)	96 ± 6	80 ± 11	91 ± 12	0.006	0.880	0.084
HR (b/min)	50 ± 5	72 ± 13	63 ± 7	<0.001	0.013	0.060
SV (mL)	58 ± 10	97 ± 20	117 ± 24	<0.001	<0.001	0.074
$\dot{Q}$ (L/min)	5.50 ± 0.97	6.87 ± 0.81	7.28 ± 1.33	0.022	0.002	1.000
TPR (mmHg/L/min)	17.73 ± 2.52	11.79 ± 1.68	12.77 ± 2.40	<0.001	<0.001	1.000

Values are mean ± SD; CMS-/CMS+, highlanders without/with chronic mountain sickness (CMS); BMI, body mass index; Hb, hemoglobin; Hct, hematocrit; SaO_2, arterial oxyhemoglobin saturation; caO_2, arterial oxygen content; PET_{O2}, end-tidal partial pressure of oxygen; PET_{CO2}, end-tidal partial pressure of carbon dioxide; SBP, systolic blood pressure; DBP, diastolic blood pressure; MAP, mean arterial pressure; HR, heart rate; SV, stroke volume; $\dot{Q}$, cardiac output; TPR, total peripheral resistance.

Table 2. Dietary intake

Group:	Lowlanders	Highlanders		*P* values			Guidelines	
Subgroup:	Controls (n = 10)	CMS- (n = 10)	CMS+ (n = 10)	CMS- *vs*. Controls	CMS+ *vs*. Controls	CMS+ *vs*. CMS-	UK	Bolivia
Energy & macronutrients								
Energy (Kcal)	2300 ± 287	2292 ± 499	2299 ± 584	0.999 (between groups)			2581 Kcal	2648 Kcal
Protein (%)	17 ± 3	15 ± 4	18 ± 4	0.355 (between groups)			15 %	10-15 %
Carbohydrate (%)	49 ± 10	55 ± 12	50 ± 10	0.361 (between groups)			50 %	55-65 %
Total fat (%)	34 ± 9	30 ± 10	31 ± 14	0.741 (between groups)			≤35 %	25-30 %
Saturated fat (%)	11 ± 5	11 ± 4	10 ± 4	0.728 (between groups)			≤ 10 %	≤ 10 %
Free sugars (%)	9 ± 4	8 ± 4	9 ± 5	0.905 (between groups)			≤ 5 %	< 10 %
Fibre (%)	20 ± 5	21 ± 8	16 ± 8	0.282 (between groups)			30 g	20-30 g
Fruit & vegetables								
Fruits (g)	424 ± 166	240 ± 147	199 ± 125	0.028	0.006	1.000	160-400 g	160-400 g
Vegetables (g)	389 ± 123	299 ± 111	160 ± 93	0.237	<0.001	0.025	160-400 g	160-480 g
Vitamins								
Vitamin C (mg)	87 ± 15	66 ± 35	36 ± 16	0.175	<0.001	0.026	40 mg	50 mg
Vitamin E (mg)	9.01 ± 1.71	4.64 ± 1.46	3.22 ± 1.57	<0.001	<0.001	0.169	>4 mg**	ND
Carotene* (µg)	4.10 ± 1.27	2.45 ± 1.30	2.15 ± 1.19	0.020	0.005	1.000	>9 mg**	ND
Minerals								
Magnesium (mg)	386 ± 83	279 ± 68	261 ± 107	0.033	0.011	1.000	300 mg	ND
Selenium (µg)	57 ± 20	51 ± 16	56 ± 20	0.742 (between groups)			75 µg	ND
Retinol (µg)	421 ± 299	191 ± 102	216 ± 126	0.042	0.081	1.000	700 µg	600 µg
Iron (mg)	14.26 ± 2.89	13.27 ± 3.30	12.52 ± 3.54	0.498 (between groups)			8.70 mg	10-28 mg
Copper (mg)	1.24 ± 0.57	1.41 ± 0.32	1.17 ± 0.32	0.444 (between groups)			1.20 mg	ND

Values are mean ± SD. Guidelines based on British [54] and Bolivian [55] reference values. *Sum of α/β-carotene and cryptoxanthins. *No Reference Nutrient Intake set, recommendation expressed as Safe Intake [54]. ND, not determined.

Table 3. Systemic arterial function and structure

Group:	**Lowlanders**	**Highlanders**		***P* values**		
Subgroup:	**Controls (n = 10)**	**CMS- (n = 10)**	**CMS+ (n = 10)**	**CMS- *vs*. Controls**	**CMS+ *vs*. Controls**	**CMS+ *vs*. CMS-**
Function						
Baseline diameter (mm)	4.69 ± 0.70	4.20 ± 0.33	4.64 ± 0.69	0.162 (between groups)		
Absolute FMD (%)	7.7 ± 2.5	5.4 ± 1.2	3.8 ± 1.1	0.017	<0.001	0.142
Adjusted FMD (%)	7.9 ± 1.3	4.9 ± 1.6	4.0 ± 1.3	<0.001 (between groups)		
GTN, Δ diameter (%)	NA	11.9 ± 2.7	8.8 ± 2.0	NA	NA	0.010
Stiffness						
Central SBP (mm Hg)	101 ± 9	126 ± 10	124 ± 10	<0.001	<0.001	1.000
Central DBP (mm Hg)	90 ± 17	76 ± 6	76 ± 8	0.040	0.040	1.000
aPWV (m/s)	7.13 ± 0.73	8.87 ± 1.24	10.26 ± 1.58	0.011	<0.001	0.043
AIx-75 (%)	17 ± 6	21 ± 7	23 ± 9	0.145 (between groups)		
Structure						
cIMT (mm)	NA	0.64 ± 0.12	0.74 ± 0.12	NA	NA	0.035

Values are mean ± SD. FMD, flow-mediated dilation; GTN, glyceryl tri-nitrate; SBP, systolic blood pressure; DBP, diastolic blood pressure; aPWV, aortic pulse wave velocity; AIx-75, augmentation index normalised to heart rate of 75 b/min; Δ, change relative to baseline; cIMT, carotid intima-media thickness; NA, not assessed.

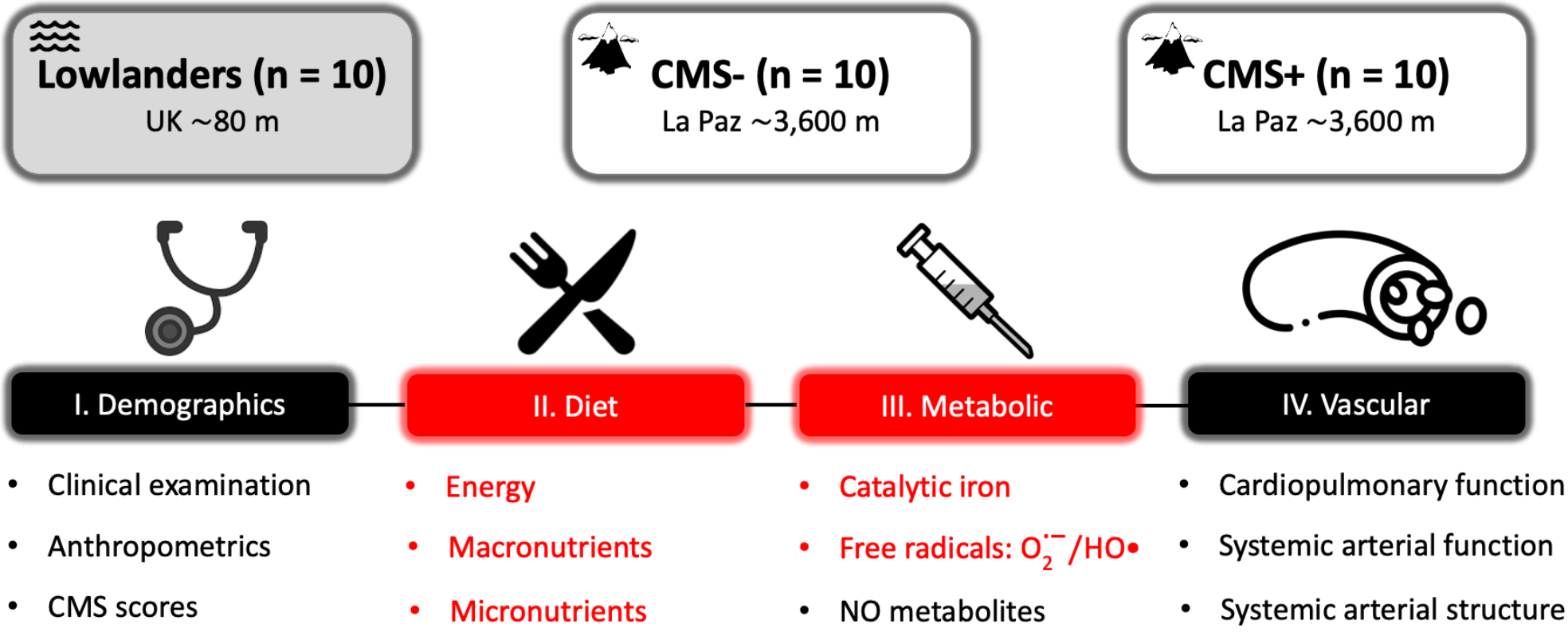
Lowlanders (n = 10)
UK ~80 m
CMS- (n = 10)
La Paz ~3,600 m
CMS+ (n = 10)
La Paz ~3,600 m
I. Demographics
II. Diet
III. Metabolic
IV. Vascular
• Clinical examination
• Anthropometrics
• CMS scores
• Energy
• Macronutrients
• Micronutrients
• Catalytic iron
• Free radicals: $O_2^{\bullet -}$/HO•
• NO metabolites
• Cardiopulmonary function
• Systemic arterial function
• Systemic arterial structure

Figure 1.

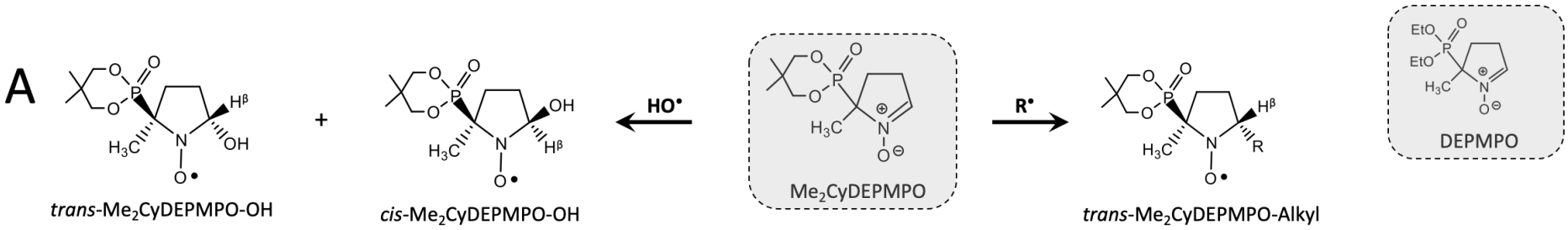
A
trans-Me2CyDEPMPO-OH
+
cis-Me2CyDEPMPO-OH
HO•
Me2CyDEPMPO
R•
trans-Me2CyDEPMPO-Alkyl
DEPMPO

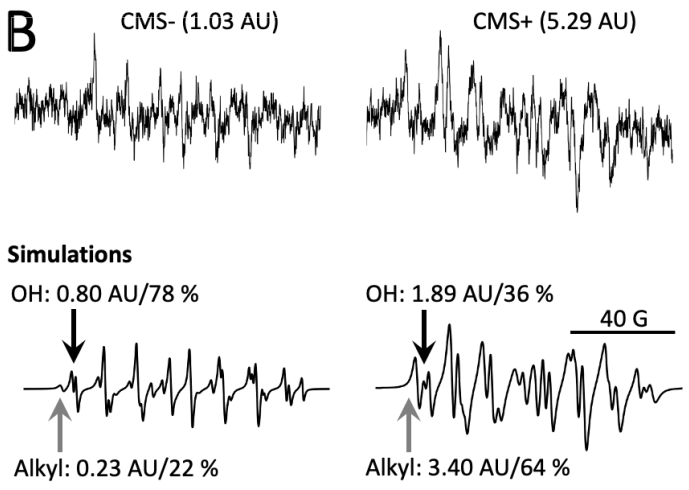
B
CMS- (1.03 AU)
CMS+ (5.29 AU)
Simulations
OH: 0.80 AU/78 %
Alkyl: 0.23 AU/22 %
OH: 1.89 AU/36 %
Alkyl: 3.40 AU/64 %
40 G

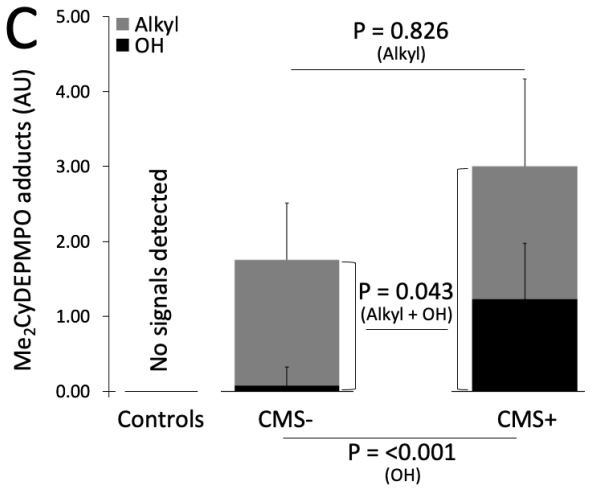
C
Alkyl
OH
Me2CyDEPMPO adducts (AU)
No signals detected
P = 0.826
(Alkyl)
P = 0.043
(Alkyl + OH)
P = <0.001
(OH)
Controls
CMS-
CMS+

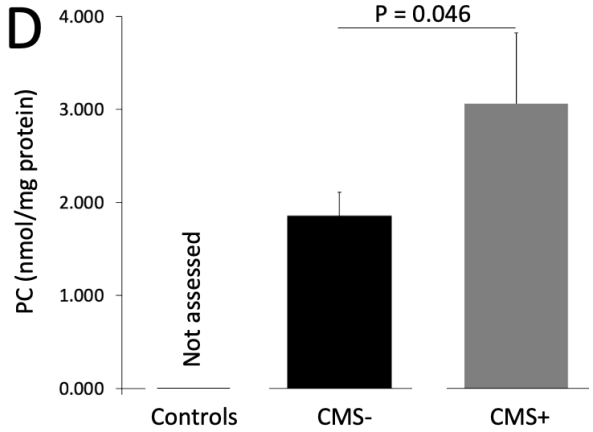
D
PC (nmol/mg protein)
Not assessed
P = 0.046
Controls
CMS-
CMS+

Figure 2.

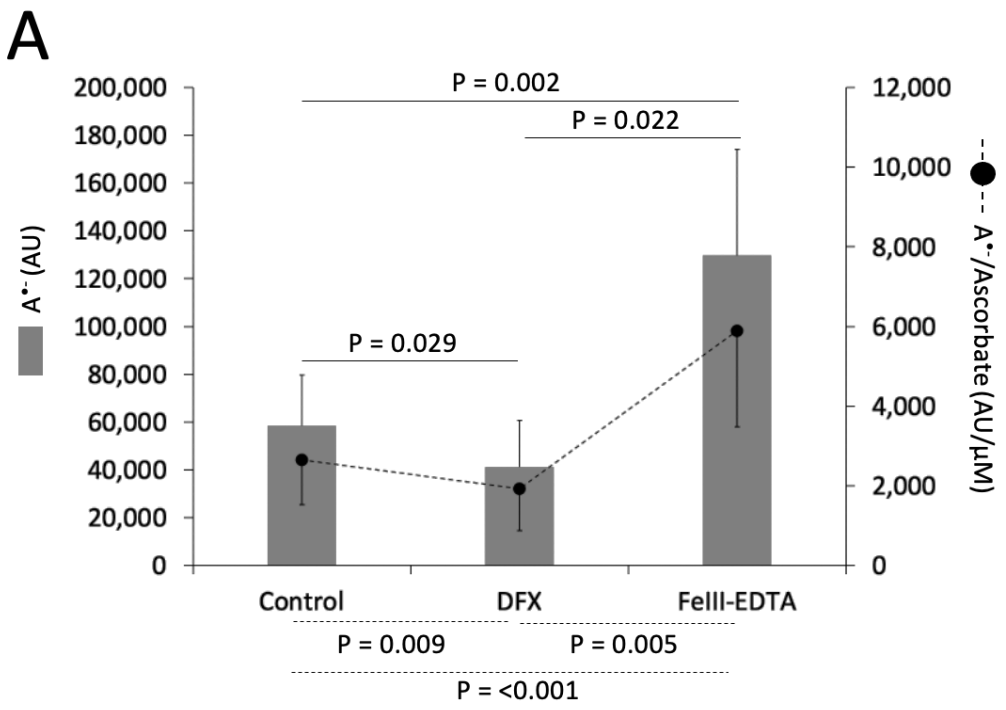
A
200,000
180,000
160,000
140,000
120,000
100,000
80,000
60,000
40,000
20,000
0
A•- (AU)
12,000
10,000
8,000
6,000
4,000
2,000
0
A•-/Ascorbate (AU/µM)
P = 0.002
P = 0.022
P = 0.029
Control
DFX
FeIII-EDTA
P = 0.009
P = 0.005
P = <0.001

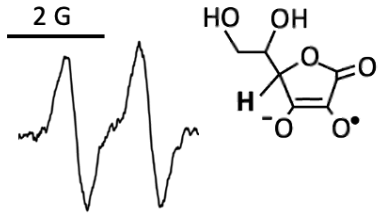
2 G
HO
OH
O
O
H
-O
O•

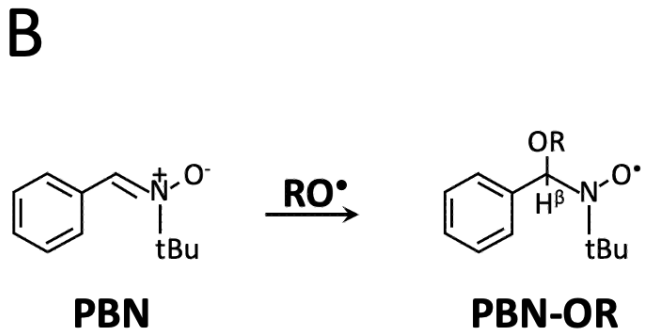
B
RO•
OR
Hβ
tBu
tBu
PBN
PBN-OR

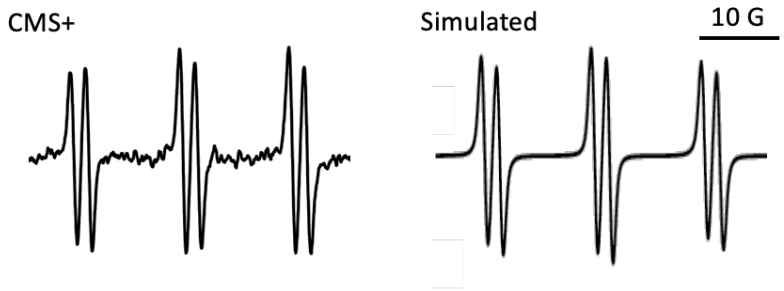
C
CMS+
Simulated
10 G

Figure 3.

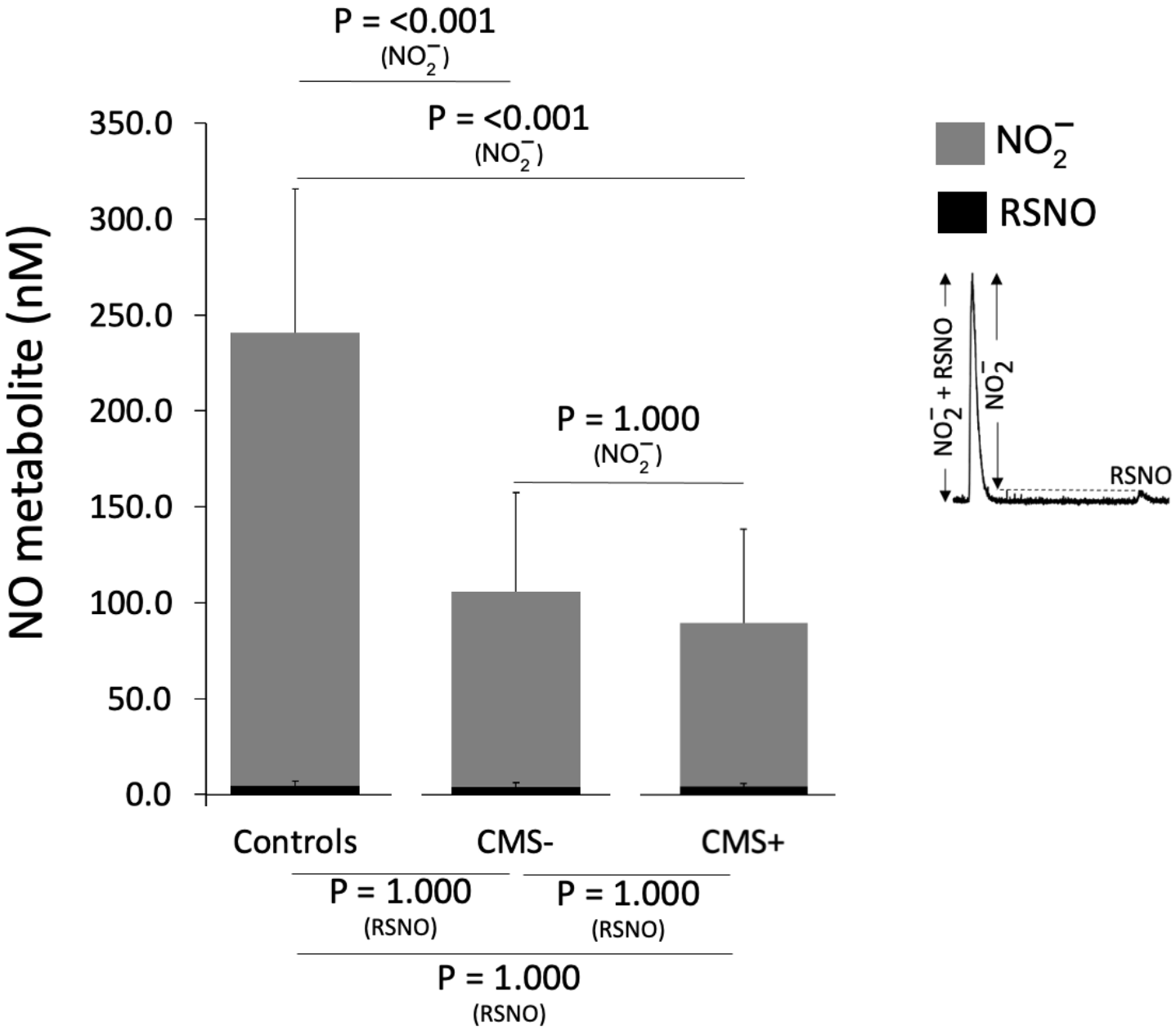
P = <0.001
(NO2−)
P = <0.001
(NO2−)
P = 1.000
(NO2−)
NO metabolite (nM)
350.0
300.0
250.0
200.0
150.0
100.0
50.0
0.0
Controls
CMS-
CMS+
P = 1.000
(RSNO)
P = 1.000
(RSNO)
P = 1.000
(RSNO)
NO2−
RSNO
NO2− + RSNO
NO2−
RSNO

Figure 4.

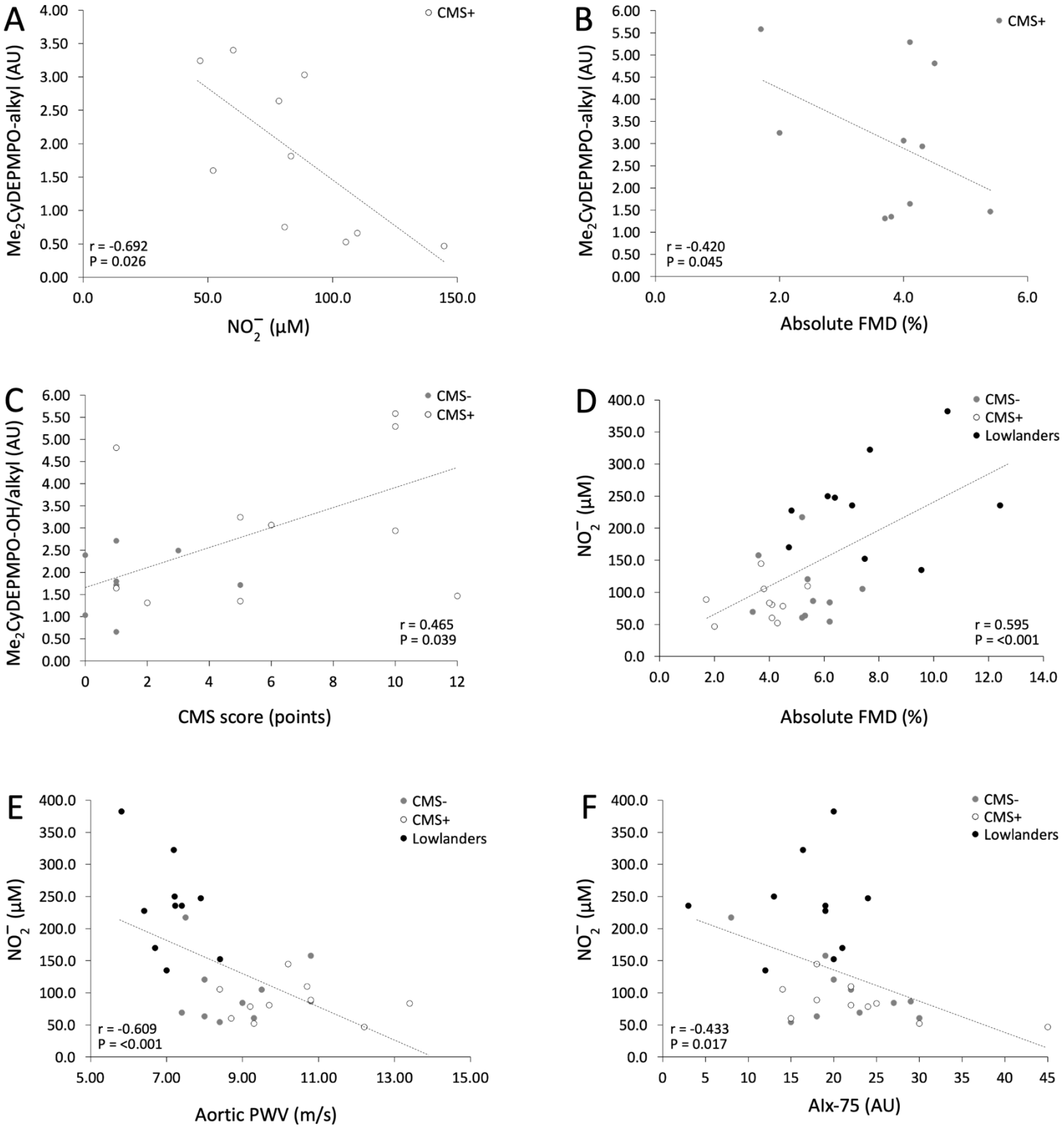
A
Me2CyDEPMPO-alkyl (AU)
NO2− (μM)
CMS+
r = -0.692
P = 0.026
B
Me2CyDEPMPO-alkyl (AU)
Absolute FMD (%)
CMS+
r = -0.420
P = 0.045
C
Me2CyDEPMPO-OH/alkyl (AU)
CMS score (points)
CMS-
CMS+
r = 0.465
P = 0.039
D
NO2− (μM)
Absolute FMD (%)
CMS-
CMS+
Lowlanders
r = 0.595
P = <0.001
E
NO2− (μM)
Aortic PWV (m/s)
CMS-
CMS+
Lowlanders
r = -0.609
P = <0.001
F
NO2− (μM)
AIx-75 (AU)
CMS-
CMS+
Lowlanders
r = -0.433
P = 0.017

Figure 5.

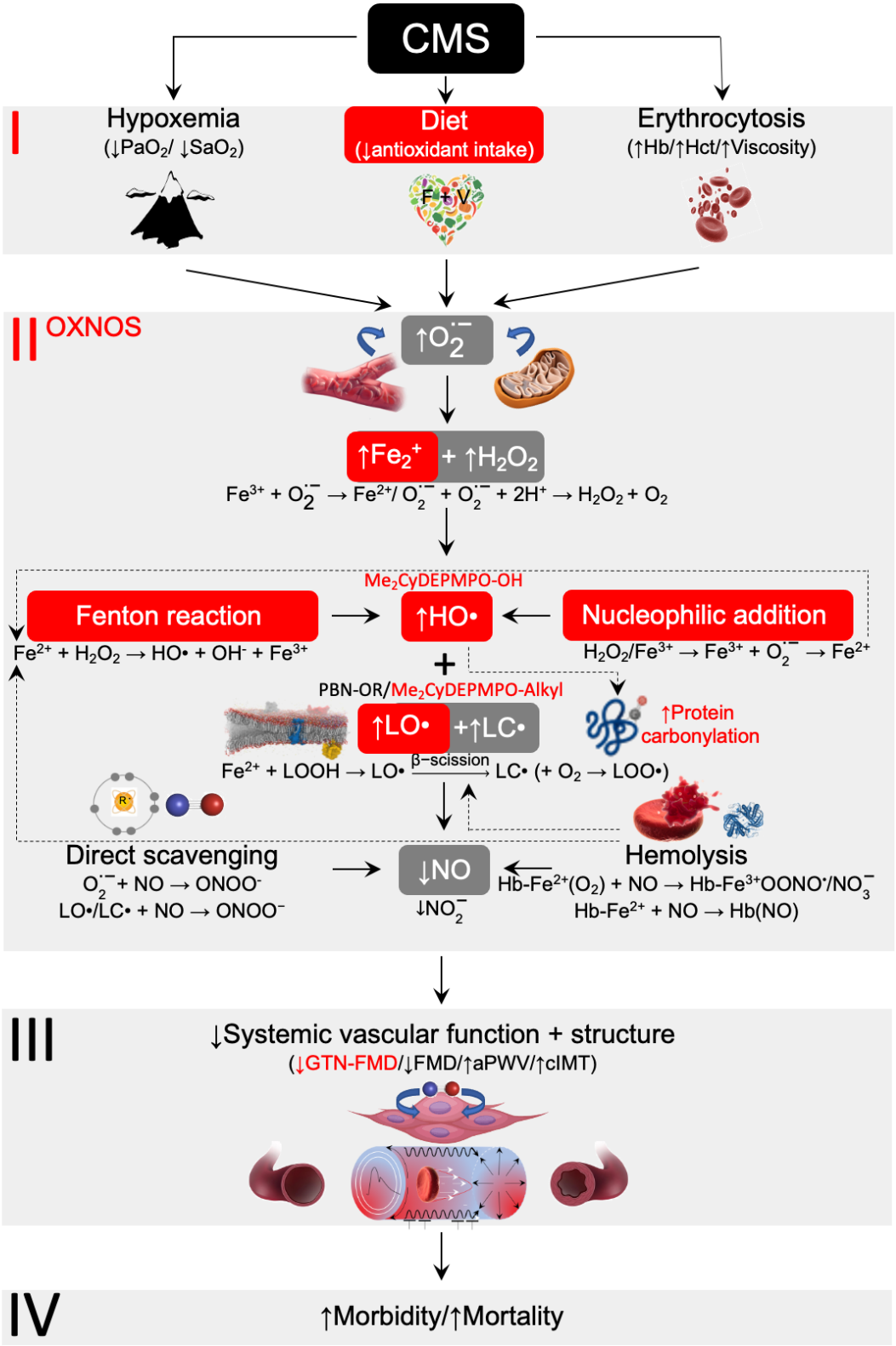
CMS
I
Hypoxemia
(↓PaO2/ ↓SaO2)
Diet
(↓antioxidant intake)
Erythrocytosis
(↑Hb/↑Hct/↑Viscosity)
II OXNOS
↑O2•−
↑Fe2+ + ↑H2O2
Fe3+ + O2•− → Fe2+/ O2•− + O2•− + 2H+ → H2O2 + O2
Me2CyDEPMPO-OH
Fenton reaction
↑HO•
Nucleophilic addition
Fe2+ + H2O2 → HO• + OH- + Fe3+
H2O2/Fe3+ → Fe3+ + O2•− → Fe2+
PBN-OR/Me2CyDEPMPO-Alkyl
↑LO• +↑LC•
↑Protein carbonylation
Fe2+ + LOOH → LO• β−scission LC• (+ O2 → LOO•)
Direct scavenging
O2•− + NO → ONOO-
LO•/LC• + NO → ONOO−
↓NO
↓NO2−
Hemolysis
Hb-Fe2+(O2) + NO → Hb-Fe3+OONO•/NO3−
Hb-Fe2+ + NO → Hb(NO)
III
↓Systemic vascular function + structure
(↓GTN-FMD/↓FMD/↑aPWV/↑cIMT)
IV
↑Morbidity/↑Mortality

Figure 6.

Supplementary data

Table S1. Hyperfine coupling constants (in Gauss) of hydroxyl and methyl radicals adducts during MeβCD[a]-assisted Me_2CyDEPMPO[b] (30 mM) spin-trapping

	***cis*-Me_2CyDEPMPO-OH**			***trans*-Me_2CyDEPMPO-OH**			***trans*-Me_2CyDEPMPO-Alkyl**		
	a_N	a_P	a_H^{β}	a_N	a_P	a_H^{β}	a_N	a_P	a_H^{β}
No MeβCD added	13.93	50.59	14.08	13.94	48.89	12.40	14.46	50.79	20.86
MeβCD after Fenton	13.91	50.55	14.22	13.93	48.81	12.45	14.09	50.43	20.80
MeβCD before Fenton	13.94	50.56	14.20	13.86	48.63	12.58	14.14	50.52	20.60
Fenton + DMSO							14.42	47.94	20.20[c]
MeβCD before Fenton							15.11	49.56	21.10

EPR spectra were acquired in 20 mM PBS (pH 7.4) 2 min after added iron. [a]Methyl-β-cyclodextrin (30 mM). [b]All chemical structures illustrated in Fig. 1A. [c]assigned to *trans*-Me_2CyDEPMPO-Me adduct according to [1].

Table S2. Iron metabolism

Group:	**Lowlanders**	**Highlanders**		***P* values**		
Subgroup:	**Controls (n = 28)**	**CMS- (n = 95)**	**CMS+ (n = 63)**	**CMS- *vs*. Controls**	**CMS+ *vs*. Controls**	**CMS+ *vs*. CMS-**
Demographics						
Age (y)	56 ± 6	56 ± 6	56 ± 5	0.361 (between groups)		
Mass (kg)	79.1 ± 9.6	65.6 ± 7.1	68.1 ± 9.2	<0.001	<0.001	0.189
Stature (m)	1.70 ± 0.05	1.60 ± 0.05	1.60 ± 0.06	<0.001	<0.001	1.000
BMI (kg/m^2)	27 ± 4	26 ± 3	27 ± 3	0.011	0.639	0.103
Clinical						
Hb (g/dL)	14.6 ± 0.9	17.9 ± 1.1	22.7 ± 1.3	<0.001	<0.001	<0.001
Hct (%)	44 ± 3	54 ± 3	68 ± 5	<0.001	<0.001	<0.001
SaO_2 (%)	97 ± 1	88 ± 3	83 ± 4	<0.001	<0.001	<0.001
caO_2 (mg/dL)	20.0 ± 1.3	21.8 ± 1.4	22.7 ± 1.3	<0.001	<0.001	<0.001
CMS score (points)	1 ± 1	2 ± 2	9 ± 4	0.211	<0.001	<0.001
Iron metabolism						
Total iron (µg/dL)	90 ± 26	107 ± 44	101 ± 58	0.274 (between groups)		
Ferritin (µg/dL)	161 ± 99	180 ± 235	138 ± 172	0.311 (between groups)		
Transferrin (mg/dL)	319 ± 48	305 ± 78	304 ± 70	0.418 (between groups)		
TSAT (%)	21 ± 7	26 ± 12	26 ± 14	0.067 (between groups)		
TIBC (µg/dL)	450 ± 67	422 ± 106	426 ± 94	0.417 (between groups)		

Values are mean ± SD; CMS-/CMS+, Highlanders without/with chronic mountain sickness; BMI, body mass index; Hb, hemoglobin; Hct, hematocrit; SaO_2, arterial oxyhemoglobin saturation; caO_2, arterial oxygen content; TSAT, trasnferrin saturation; TIBC, total iron binding capacity.

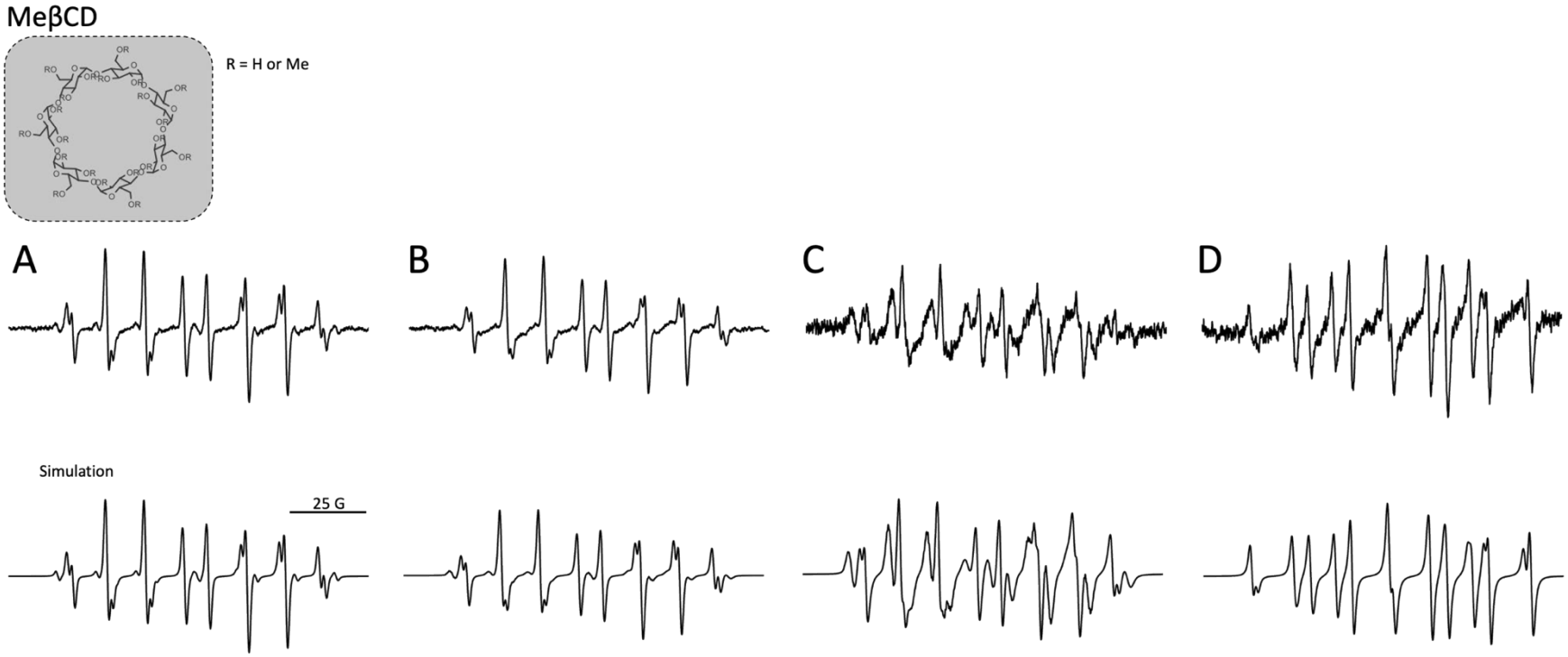

Fig. S1. Typical EPR signals showing the effect of MeβCD on Me_2CyDEPMPO hydroxyl and methyl radicals spin adducts.

Spectra were obtained by reacting the nitrone (30 mM) with a Fenton reagent consisting of hydrogen peroxide (1 mM) and $FeSO_4$ (1 mM) in PBS (20 mM; pH 7.4) in the absence (A) or presence (B−D) of MeβCD (50 mM). Cyclodextrin (CD) was added 30 s before (C) or after (B, D) addition of iron. Signal D was obtained as for (B, C) except that buffer contained 10% v/v DMSO. Single-scan spectra (2-k points resolution) were acquired at room temperature 2 min after addition of iron using the instrument settings: microwave power, 10 mW; modulation amplitude, 0.521 G; gain, 2×10^5; time constant, 81.92 ms; sweep rate, 1.55 G/s for a sweep width of 130 G. Simulations of A-C were consistent with mixtures of *cis/trans*-OH and alkyl radical adducts (see Fig. 1B for labeling of characteristic lines), while trace D was consistent with a mixture of 24% *trans*-Me_2CyDEPMPO-Me and an unassigned 76% Me_2CyDEPMPO-alkyl adduct. Vertical scale for (C, D: $\pm 5 \times 10^3$ AU) compressed 4-fold relative to (A, B: $\pm 20 \times 10^3$ AU). Inset: General structure of MeβCD.

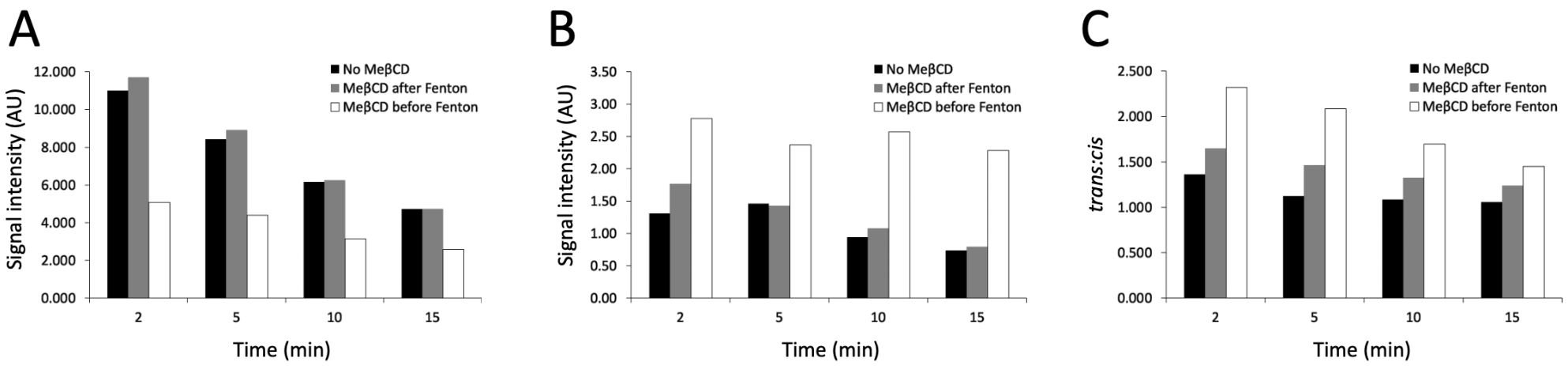

Fig. S2. Effect of MeβCD on spin trapping kinetics and diastereoisomeric ratios of Me_2CyDEPMPO adducts in the non-stopped Fenton generating system.

Aggregate concentrations of (A) *cis*/*trans* hydroxyl radical adducts and (B) alkyl adducts concentrations. (C) *Trans*-OH/*cis*-OH ratios. Samples preparation and EPR acquisition were as described in the legend of Fig.S1. Time refers to iron addition to the Fenton reagent.

References

[1] G. Gosset, J.L. Clément, M. Culcasi, A. Rockenbauer, S. Pietri, CyDEPMPOs: a class of stable cyclic DEPMPO derivatives with improved properties as mechanistic markers of stereoselective hydroxyl radical adduct formation in biological systems, Bioorganic and Medicinal Chemistry 19(7) (2011) 2218-30.